Asymmetric collision of two shock waves in AdS_5

JHEP05(2009)060

(http://iopscience.iop.org/1126-6708/2009/05/060)

Published by IOP Publishing for SISSA

Received: *February 27, 2009*
Revised: *April 7, 2009*
Accepted: *April 20, 2009*
Published: *May 14, 2009*

Asymmetric collision of two shock waves in AdS_5

Javier L. Albacete,[a] **Yuri V. Kovchegov**[b] **and Anastasios Taliotis**[b]

[a] *ECT*,*
Strada delle Tabarelle 286, I-38050, Villazzano (TN), Italy
[b] *Department of Physics, The Ohio State University,*
Columbus, OH 43210, U.S.A.
E-mail: albacete@mps.ohio-state.edu, yuri@mps.ohio-state.edu, taliotis.1@osu.edu

Abstract: We consider high energy collisions of two shock waves in AdS_5 as a model of ultrarelativistic nucleus-nucleus collisions in the boundary theory. We first calculate the graviton field produced in the collisions in the NLO and NNLO approximations, corresponding to three- and four-graviton exchanges with the shock waves. We then consider the asymmetric limit where the energy density in one shock wave is much higher than in the other one. In the boundary theory this setup corresponds to proton-nucleus collisions, with the nucleus being the denser of the two shock waves and the proton being the less dense one. Employing the eikonal approximation we find the exact high energy analytic solution for the metric in AdS_5 for the asymmetric collision of two delta-function shock waves. The solution resums all-order graviton exchanges with the "nucleus" shock wave and a single-graviton exchange with the "proton" shock wave. Using the holographic renormalization prescription we read off the energy-momentum tensor of the matter produced in proton-nucleus collisions. We show in explicit detail that in the boundary theory the proton is completely stopped by strong-coupling interactions with the nucleus, in agreement with our earlier results [1]. We also apply the eikonal technique to the asymmetric collision of two unphysical delta-prime shock waves, which we introduced in [1] as a means of modeling nuclear collisions with weak coupling initial dynamics. We obtain a surprising result that, for delta-prime shock waves, the multiple bulk graviton exchange series giving the leading energy-dependent contribution to the energy-momentum tensor terminates at the order of two graviton exchanges with the nucleus.

Keywords: Gauge-gravity correspondence, AdS-CFT Correspondence, Hadronic Colliders, QCD

ArXiv ePrint: 0902.3046

doi:10.1088/1126-6708/2009/05/060

JHEP05(2009)060

Contents

JHEP05(2009)060

1 Introduction

In this paper we continue our earlier investigation [1] of colliding shock waves in AdS_5. Due to the Anti-de Sitter space/conformal field theory (AdS/CFT) correspondence [2–5], the problem of two colliding gravitational shock waves, while an important problem from the standpoint of gravity theory [6–9], may also be relevant for high energy hadronic and nuclear collisions at strong coupling [10–14].

One of the most important problems in the field of ultrarelativistic heavy ion collisions is the one of isotropization and thermalization of the produced medium. There is a growing consensus in the heavy ion community that the medium produced in heavy ion collisions

at RHIC is strongly coupled [15–23]. The challenge for the theoretical community is to understand

(i) how the medium, which is initially very anisotropic with zero or negative longitudinal component of the energy-momentum tensor [24–29], evolves into an isotropic medium described by ideal (Bjorken [30]) hydrodynamics, and

(ii) why this transition happens over extremely short time scale of $0.3 \div 0.6\,\mathrm{fm/c}$, as required by hydrodynamic simulations [15–22].

There is also a widespread belief in the community, supported by a broad range of phenomenological evidence, that the very early stages of heavy ion collisions are weakly-coupled, i.e., they are described by the physics of Color Glass Condensate (CGC)/parton saturation [24, 26, 31–47] (for a review of CGC see [48–50]). It appears that the system produced in heavy ion collisions evolves with time from the weakly-coupled CGC state to the strongly coupled quark-gluon plasma (QGP) described by the ideal hydrodynamics. There are two types of transitions that the system has to undergo in order for such process to take place. First of all, at some point in time the system should undergo a transition from weak coupling to strong coupling. Second of all, at a (presumably) different time the system will evolve from the anisotropic early state, in which transverse and longitudinal pressure components in the energy-momentum tensor are drastically different, to the isotropic later state, in which all pressure components are equal (or almost equal) to each other, as required by the ideal (viscous) hydrodynamics. We will refer to the latter transition as the *isotropization transition*. The isotropization transition is a necessary condition for the thermalization of the produced medium.

In this work we will assume that the isotropization transition takes place after the strong coupling transition. Hence we will study the onset of the isotropization in the strongly-coupled framework. Since strong coupling dynamics in QCD is prohibitively complicated, especially for the ultrarelativistic processes at hand, we will employ AdS/CFT correspondence, assuming that the bulk properties of the collisions and the produced medium in $\mathcal{N} = 4$ super-Yang-Mills theory are not too different from QCD and would allow us to make conclusions which are at least qualitatively applicable to the real life.

Attempts to study isotropization and thermalization in the AdS/CFT framework have been made before. A gravity-dual of Bjorken hydrodynamics was constructed in [51–55]. To obtain it the authors of [51] assumed that the medium produced in heavy ion collisions is rapidity-independent. Imposing a no-singularities requirement [51] (or simply demanding that the metric is real [28]) one then obtains the asymptotic late-time geometry corresponding to Bjorken hydrodynamics. However, this result by itself does not prove that Bjorken hydrodynamics is a consequence of a heavy ion collision. In other words, it is not clear which early-time dynamics (or, in general, which events in the past) lead to this dual-Bjorken geometry.

To address this problem, by analogy with the perturbative approaches [24, 25, 37, 56], it was suggested in [10] that one should study collisions of two shock waves in AdS space: following the dynamics of the strongly-coupled medium produced in such collisions one would

JHEP05(2009)060

be able to see how the ideal hydrodynamic state is reached by the medium and whether this late-time state is rapidity-independent. In [11] the case of shock wave collisions in the $1+1$ dimensional boundary theory was considered and solved exactly in AdS_3 geometry. Unfortunately the lower dimensionality of the problem severely limits the physical behavior of the produced medium, and does not allow to formulate the problem of isotropization. The case of realistic $1+3$ boundary theory was first addressed in [12] using AdS_5 space with the infinitely-thin delta-function shock waves. The authors of [12] constructed a perturbative series for the energy-momentum tensor of the produced strongly coupled matter.

In [1] we generalized the results of [12] by solving Einstein equations in a more general framework, which does not depend on the exact profile of the shock waves, i.e., whether they are delta-functions or some other objects with finite extent. We identified the perturbation series of [12] with a series in bulk graviton exchanges with two shock waves (see e.g. figure 2 below for an example of a term contributing to the series). Most importantly, in [1] it was argued that in a collision of any two physical shock waves, they stop shortly after the collision, possibly forming a black hole. In the boundary theory this behavior corresponds to the colliding nuclei stopping shortly after the collision, probably leading to Landau hydrodynamics description of the system [57]. Such complete nuclear stopping would lead to complete stopping of the baryon number carried by the nuclei. As such a complete baryon stopping is not observed at RHIC (and, in fact, baryon stopping at mid-rapidity at RHIC is rather small [58] in accord with perturbative calculations [59, 60]), this indicates that colliding shock waves may not be adequate for the description of realistic nuclear collisions in AdS. Indeed, an AdS description would apply if the collisions were strongly-coupled at all times: as the early stages of RHIC heavy ion collisions are weakly coupled, an AdS/CFT description of the collision at all times can not be valid. In an attempt to resolve the issue we suggested in [1] that one could use unphysical shock waves with the delta-prime profile. Such shock waves appear to have no stopping. It is possible that using delta-prime shock waves as external sources for the AdS/CFT correspondence would yield a more realistic description of heavy ion collisions, and would allow one to tackle the problem of isotropization in the strongly-coupled framework.

In this paper we further explore shock wave collisions. In section 2 we extend the expansion in graviton exchanges from [1] to two higher orders. We calculate the next-to-leading order (NLO) and next-to-next-to-leading order (NNLO) corrections to the result of [1] for both delta-function and delta-prime shock waves (see eqs. (2.30 and (2.35), along with eq. (2.39)).

We continue in section 3 by constructing the resummation procedure in which graviton exchanges with one shock wave are resummed to all orders while the interaction with another shock wave is restricted to a single graviton exchange (see figure 6 below). The diagrams are analogous to those resummed in the study of classical gluon fields produced in proton-nucleus collisions in the perturbative CGC framework [61–65] (see [50] for a review). We apply the eikonal approximation to Einstein equations, which allows us to construct an exact solution for the energy-momentum tensor of the produced medium in the case of delta-function shock waves, given in eq. (3.38). (Eikonal approximation in AdS/CFT was studied before in [66–70]). Our solution would receive energy-suppressed corrections

JHEP05(2009)060

if shock waves of finite width are considered. We note that the energy-momentum tensor (3.38) is not that of ideal hydrodynamics, indicating that the system does not reach isotropization/thermalization in proton-nucleus approximation to the collision. Resumming graviton exchanges with the nucleus shock wave to all orders allows us to demonstrate the stopping of the proton shock wave explicitly. The relevant component of the energy-momentum tensor of the proton in shown in eq. (3.45): one can explicitly see that it goes to zero as the light cone coordinate x^+ (in which direction the proton was initially moving) is increasing.

We also apply the eikonal treatment to the delta-prime shock waves. The results are quite interesting: we show that in the eikonal approximation the series in graviton exchanges terminates at the level of two graviton exchanges with the nucleus shock wave. Thus the NLO result for the energy-momentum tensor is, in fact, exact for the case of proton-nucleus collisions! The energy-momentum tensor for delta-prime shock waves is shown in eq. (3.71). It is clear from eq. (3.71) that the produced medium distribution has a strong rapidity dependence. Therefore it seems unlikely that rapidity-independent Bjorken hydrodynamics geometry of [51] could result from a collision of two shock waves in AdS_5 space, though indeed a further study of the full nucleus-nucleus scattering problem is needed to unambiguously answer this question.

We will conclude in section 4 by summarizing our main results.

2 Perturbative expansion in graviton exchanges

2.1 General setup

Consider a collision of two ultrarelativistic nuclei. Assume for simplicity that the nuclei have infinite transverse extent and the same longitudinal thickness at all impact parameters. The energy-momentum tensors of the two nuclei can be written as $\langle T_{1\,--}(x^-)\rangle$ and $\langle T_{2\,++}(x^+)\rangle$ with the brackets $\langle\ldots\rangle$ denoting the averaging in the nuclear wave functions and the light cone coordinates defined by $x^\pm = (x^0 \pm x^3)/\sqrt{2}$ where x^3 is the collision axis. The geometry of the collision is shown in figure 1.

As was argued in [51], the geometry in AdS_5 dual to each one of the nuclei in the boundary theory is given by the following metric

$$ds^2 = \frac{L^2}{z^2}\left\{-2\,dx^+\,dx^- + t_1(x^-)\,z^4\,dx^{-\,2} + dx_\perp^2 + dz^2\right\} \tag{2.1}$$

for nucleus 1 and by

$$ds^2 = \frac{L^2}{z^2}\left\{-2\,dx^+\,dx^- + t_2(x^+)\,z^4\,dx^{+\,2} + dx_\perp^2 + dz^2\right\} \tag{2.2}$$

for nucleus 2. Here $dx_\perp^2 = (dx^1)^2 + (dx^2)^2$ with x^1 and x^2 the transverse dimensions which we will denote using Latin indices, e.g. x^i. L is the curvature radius of the AdS_5 space and z is the coordinate describing the 5th dimension with the boundary of the AdS space at $z = 0$. We have also defined

$$t_1(x^-) \equiv \frac{2\,\pi^2}{N_c^2}\,\langle T_{1\,--}(x^-)\rangle \tag{2.3}$$

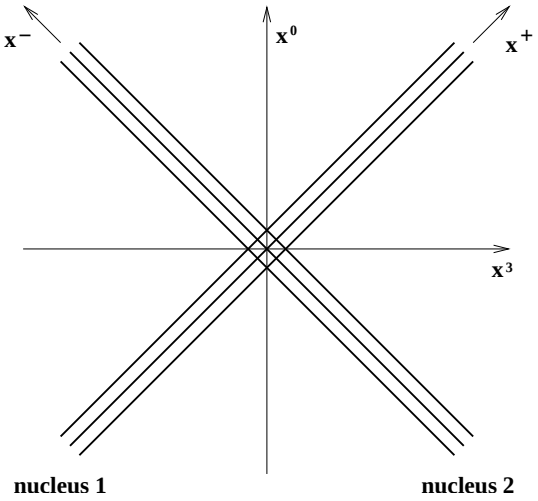

Figure 1. The space-time picture of the ultrarelativistic heavy ion collision in the center-of-mass frame. The collision axis is labeled x^3, the time is x^0.

and

$$t_2(x^+) \equiv \frac{2\,\pi^2}{N_c^2}\,\langle T_{2\,++}(x^+)\rangle \tag{2.4}$$

in accordance with the prescription of holographic renormalization [71]. The metrics in eqs. (2.1) and (2.2) are exact solutions of Einstein equations in the empty AdS_5 space

$$R_{\mu\nu} + \frac{4}{L^2}\,g_{\mu\nu} = 0. \tag{2.5}$$

Our goal is to construct the geometry in AdS_5 dual to the collision of two shock waves given by eqs. (2.1) and (2.2). In [1] we argued that the single shock wave metric in eq. (2.1) (or in eq. (2.2)) corresponds to the single-graviton exchange between the source nucleus at the boundary and the point in the bulk where the metric is measured. The solution of Einstein equations (2.5) for the collision of two shock waves can therefore be represented as a sum of tree-level graviton exchange diagrams, as shown in figure 2. There the source nuclei are represented by thick crosses, with nucleus 1 given by the crosses on the top, and nucleus 2 given by the crosses at the bottom. As was argued in [1], each rescattering in nucleus 1 brings in a factor of $t_1(x^-)$ into the metric, while each rescattering in nucleus 2 brings in a factor of $t_2(x^+)$. The large thin cross in figure 2 denotes the point in the bulk in the argument of the metric, i.e., the point where the metric is "measured". One encounters similar diagrams but with gluons and in 4 dimensions for nuclear collisions in the framework of McLerran-Venugopalan (MV) model [32–34], as was worked out in [37, 38, 41, 56, 61, 72].

Inspired by the graviton-exchange analogy of figure 2 we write the metric dual to the full collision as [1]

$$ds^2 = \frac{L^2}{z^2}\Big\{ -2dx^+dx^- + dx_\perp^2 + dz^2 + t_1(x^-)z^4dx^{-2} + t_2(x^+)z^4dx^{+2} + o(t_1t_2)\Big\}. \tag{2.6}$$

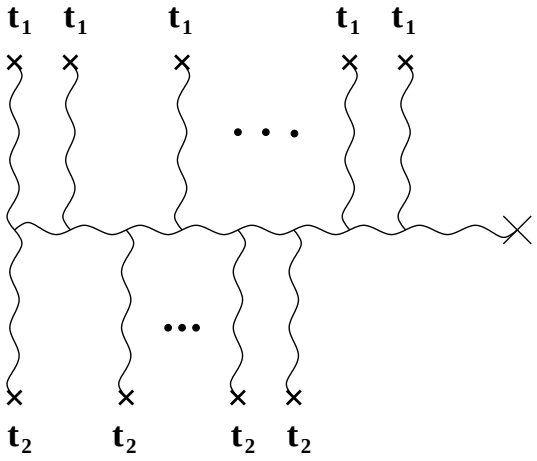

Figure 2. Diagrammatic representation of the solution of classical Einstein equations for the collisions of two shock waves. The wavy lines denote graviton exchanges between the sources at the boundary (thick crosses) and the bulk. The large cross denotes the point in the bulk where one measures the metric. The upper row of thick crosses denotes rescatterings in nucleus 1, each of which generates a factor of t_1. The lower row of thick crosses denotes rescatterings in nucleus 2, each of which generates a factor of t_2.

Indeed the interesting unknown part of the answer is in the term denoted $o(t_1\, t_2)$ in eq. (2.6): this term comprises all higher order graviton exchanges, i.e., higher powers of $t_1(x^-)$ and $t_2(x^+)$. The first term in this expansion, the term proportional to $t_1\, t_2$ was found in [1]. For a particular form of $t_1(x^-)$ and $t_2(x^+)$ given by delta-functions, the expansion to several higher orders in t_1 and t_2 was constructed in [12].

To construct a series in graviton exchanges for a general form of t_1 and t_2 and to set up the general problem we write

$$ds^2 = \frac{L^2}{z^2}\Big\{ -\left[2+G(x^+,x^-,z)\right]\, dx^+\, dx^- + \left[t_1(x^-)\, z^4 + F(x^+,x^-,z)\right]\, dx^{-\,2} + \left[t_2(x^+)\, z^4 + \tilde{F}(x^+,x^-,z)\right]\, dx^{+\,2} + [1+H](x^+,x^-,z)\, dx_\perp^2 + dz^2\Big\}. \tag{2.7}$$

The unknown functions $F(x^+,x^-,z)$, $\tilde{F}(x^+,x^-,z)$, $G(x^+,x^-,z)$, and $H(x^+,x^-,z)$ contain all higher powers of t_1 and t_2. Note that as eq. (2.1) and eq. (2.2) are exact solution of Einstein equations (2.5), the functions F, $\tilde{F}$, G, and H contain at least one power of t_1 and t_2 each [1].

Substituting the metric of eq. (2.7) into Einstein equations (2.5) yields a very complicated system of non-linear equations. It is likely that the solution of these equations is only possible numerically. Here we will build on the results of [1] to construct the first few steps of the perturbative expansion: we will construct the next-to-leading order (NLO) and the next-to-next-to-leading order (NNLO) corrections to F, $\tilde{F}$, G and H. NLO corrections resum terms containing $t_1^2 t_2$ and $t_1 t_2^2$, while NNLO corrections include terms with $t_1^3 t_2$, $t_1^2 t_2^2$ and $t_1 t_2^3$. (The powers of t_1 and t_2 should not be taken literally, they only indicate

JHEP05(2009)060

the number of times t_1 and t_2 enter the expression.) In section 3 we will use the eikonal approximation to resum one power of t_1 and *all* powers of t_2.

Before we start the calculations let us first point out that, according to the prescription of holographic renormalization [71], if we expand the unknown coefficients of the metric in eq. (2.7) into a series in powers of z^2

$$\begin{aligned} F(x^+,x^-,z) &= z^4 \sum_{n=0}^{\infty} F_n(x^+,x^-)\, z^{2n}, \quad \tilde{F}(x^+,x^-,z) = z^4 \sum_{n=0}^{\infty} \tilde{F}_n(x^+,x^-)\, z^{2n}, \\ G(x^+,x^-,z) &= z^4 \sum_{n=0}^{\infty} G_n(x^+,x^-)\, z^{2n}, \quad H(x^+,x^-,z) = z^4 \sum_{n=0}^{\infty} H_n(x^+,x^-)\, z^{2n}, \end{aligned} \tag{2.8}$$

then the expectation value of the energy-momentum tensor of the matter produced in the collision in the boundary theory is given by the first coefficients in the expansion in eq. (2.8):

$$\begin{aligned} \langle T^{++} \rangle &= \frac{N_c^2}{2\pi^2} F_0(x^+,x^-) & \langle T^{--} \rangle &= \frac{N_c^2}{2\pi^2} \tilde{F}_0(x^+,x^-) \\ \langle T^{+-} \rangle &= -\frac{1}{2}\frac{N_c^2}{2\pi^2} G_0(x^+,x^-) & \langle T^{ij} \rangle &= \frac{N_c^2}{2\pi^2} \delta^{ij} H_0(x^+,x^-). \end{aligned} \tag{2.9}$$

Einstein equations (2.5) impose two constraints on the energy-momentum tensor: tracelessness

$$\langle T_\mu{}^\mu \rangle = 0 \tag{2.10}$$

and energy-momentum conservation

$$\partial_\nu \langle T^{\mu\nu} \rangle = 0. \tag{2.11}$$

Imposing the constraints (2.10) and (2.11) on the energy-momentum tensor in eq. (2.9) we easily see that the energy-momentum tensor can be expressed in terms of a single unknown function:

$$\begin{aligned} \langle T^{++} \rangle &= -\frac{N_c^2}{2\pi^2}\frac{\partial_-}{\partial_+} H_0(x^+,x^-) & \langle T^{--} \rangle &= -\frac{N_c^2}{2\pi^2}\frac{\partial_+}{\partial_-} H_0(x^+,x^-) \\ \langle T^{+-} \rangle &= \frac{N_c^2}{2\pi^2} H_0(x^+,x^-) & \langle T^{ij} \rangle &= \frac{N_c^2}{2\pi^2} \delta^{ij} H_0(x^+,x^-). \end{aligned} \tag{2.12}$$

Here we defined the following integrations

$$\frac{1}{\partial_+}[\ldots](x^+) \equiv \int_{-\infty}^{x^+} dx'^+ [\ldots](x'^+), \quad \frac{1}{\partial_-}[\ldots](x^-) \equiv \int_{-\infty}^{x^-} dx'^- [\ldots](x'^-). \tag{2.13}$$

Eqs. (2.12) demonstrate that only one metric coefficient in (2.7) is needed to construct the energy-momentum tensor of the produced matter in the boundary theory.

JHEP05(2009)060

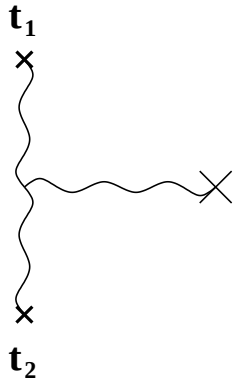

Figure 3. Graviton diagram corresponding to the LO solution of Einstein equations found in [1].

2.2 NLO results

2.2.1 NLO calculation

To systematically include the graviton exchanges of figure 2 into the metric of eq. (2.7) we expand the coefficients of the metric in powers of t_1 and t_2. We start by writing

$$\begin{aligned}
F(x^+,x^-,z) &= F^{(0)}(x^+,x^-,z) + F^{(1)}(x^+,x^-,z) + F^{(2)}(x^+,x^-,z) + \cdots \\
\tilde{F}(x^+,x^-,z) &= \tilde{F}^{(0)}(x^+,x^-,z) + \tilde{F}^{(1)}(x^+,x^-,z) + \tilde{F}^{(2)}(x^+,x^-,z) + \cdots \\
G(x^+,x^-,z) &= G^{(0)}(x^+,x^-,z) + G^{(1)}(x^+,x^-,z) + G^{(2)}(x^+,x^-,z) + \cdots \\
H(x^+,x^-,z) &= H^{(0)}(x^+,x^-,z) + H^{(1)}(x^+,x^-,z) + H^{(2)}(x^+,x^-,z) + \cdots
\end{aligned} \tag{2.14}$$

where the superscript (0) denotes terms containing $t_1\,t_2$, i.e., quadratic in t's, the superscript (1) denotes terms cubic in t's (i.e., terms containing $t_1^2\,t_2$ and $t_1\,t_2^2$), the superscript (2) denotes terms quadric in t's, etc. Note that the expansion in t's in eq. (2.14) is independent of the expansion in z's in eq. (2.8): each term in the expansion in eq. (2.14) can in turn be expanded in powers of z^2 as was done in eq. (2.8), and vice versa.

The leading order (LO) terms in eq. (2.14) denoted by the superscript (0) were found in [1]. For completeness let us quote the results here:

$$\begin{aligned}
F^{(0)}(x^+,x^-,z) &= -\lambda_1(x^+,x^-)\,z^4 - \frac{1}{6}\,\partial_-^2 h_0(x^+,x^-)\,z^6 - \frac{1}{16}\,\partial_-^2 h_1(x^+,x^-)\,z^8 \\
\tilde{F}^{(0)}(x^+,x^-,z) &= -\lambda_2(x^+,x^-)\,z^4 - \frac{1}{6}\,\partial_+^2 h_0(x^+,x^-)\,z^6 - \frac{1}{16}\,\partial_+^2 h_1(x^+,x^-)\,z^8 \\
G^{(0)}(x^+,x^-,z) &= -2\,h_0(x^+,x^-)\,z^4 - 2\,h_1(x^+,x^-)\,z^6 + \frac{2}{3}\,t_1(x^-)\,t_2(x^+)\,z^8 \\
H^{(0)}(x^+,x^-,z) &= h_0(x^+,x^-)\,z^4 + h_1(x^+,x^-)\,z^6.
\end{aligned} \tag{2.15}$$

We defined [1]

$$\begin{aligned}
h_0(x^+,x^-) &= \frac{8}{\partial_+^2\,\partial_-^2}\,t_1(x^-)\,t_2(x^+), & h_1(x^+,x^-) &= \frac{4}{3\,\partial_+\,\partial_-}\,t_1(x^-)\,t_2(x^+) \\
\lambda_1(x^+,x^-) &= \frac{\partial_-}{\partial_+}\,h_0(x^+,x^-), & \lambda_2(x^+,x^-) &= \frac{\partial_+}{\partial_-}\,h_0(x^+,x^-).
\end{aligned} \tag{2.16}$$

JHEP05(2009)060

The diagram corresponding to the LO solution given by eqs. (2.15) and (2.16) is shown in figure 3. Note that the z^4 terms in eq. (2.15) adhere to the pattern outlined in eqs. (2.12).

To find the NLO terms denoted by superscript (1) in eq. (2.14) we substitute the metric (2.7) with the coefficients expanded according to eq. (2.14) into Einstein equations (2.5). Expanding the Einstein equations to the cubic order in t's yields the following equations for $G^{(1)}$ and $H^{(1)}$

$$(\perp\perp) \qquad G^{(1)}_z + 5\,H^{(1)}_z - z\,H^{(1)}_{z\,z} + 2\,z\,H^{(1)}_{x^+\,x^-} + \delta_7\,z^7 + \delta_9\,z^9 + \delta_{11}\,z^{11} = 0 \tag{2.17a}$$

$$(zz) \qquad G^{(1)}_z + 2H^{(1)}_z - z\,G^{(1)}_{z\,z} - 2\,z\,H^{(1)}_{z\,z} + 48\,\alpha_7\,z^7 + 80\,\alpha_9\,z^9 + 120\,\alpha_{11}\,z^{11} = 0. \tag{2.17b}$$

The coefficients δ_7, δ_9, δ_{11}, α_7, α_9, α_{11} are known functions of t_1 and t_2 the exact form of which is not important here. The subscripts z, x^+ and x^- indicate partial derivatives with respect to these variables. Eqs. (2.17a) and (2.17b) are labeled according to the lowercase Einstein equations components.

Solving eq. (2.17a) for $G^{(1)}_z$ and substituting the result into eq. (2.17b) yields the following equation for $H^{(1)}$

$$-3\,H^{(1)}_z + 3\,z\,H^{(1)}_{z\,z} - z^2\,H^{(1)}_{z\,z\,z} + 2\,z^2\,H^{(1)}_{x^+\,x^-\,z} + 12\,\psi_7\,z^7 + 16\,\psi_9\,z^9 + 20\,\psi_{11}\,z^{11} = 0 \tag{2.18}$$

with the coefficients ψ given by

$$\begin{aligned}
\psi_7 &= \frac{4}{3}\left[t_2(x^+)\,\lambda_1(x^+,x^-) + t_1(x^-)\,\lambda_2(x^+,x^-)\right] \\
\psi_9 &= \frac{3}{4}\left[t_2(x^+)\,h_{0\;x^-\,x^-}(x^+,x^-) + t_1(x^-)\,h_{0\;x^+\,x^+}(x^+,x^-)\right] \\
\psi_{11} &= \frac{3}{5}\left[t_2(x^+)\,h_{1\;x^-\,x^-}(x^+,x^-) + t_1(x^-)\,h_{1\;x^+\,x^+}(x^+,x^-)\right].
\end{aligned} \tag{2.19}$$

To find the solution of eq. (2.18) we follow the strategy used in [1]. We first expand $H^{(1)}$ into a series in powers of z^2

$$H^{(1)}(x^+,x^-,z) \;=\; z^4 \sum_{n=0}^{\infty} H^{(1)}_n(x^+,x^-)\,z^{2\,n}. \tag{2.20}$$

Substituting eq. (2.20) into eq. (2.18) and requiring that the coefficients at each power of z on the left hand side are zero yields the recursion relation

$$H^{(1)}_n\,(-2n)\,(2+n) + H^{(1)}_{n-1;\;x^+x^-} + \psi_7\,\delta_{n,2} + \psi_9\,\delta_{n,3} + \psi_{11}\,\delta_{n,4} = 0 \qquad n \geq 1. \tag{2.21}$$

Arguing just like in [1] that causality requires the series (2.20) to terminate at some finite order, we see that the series can only be terminated if $H^{(1)}_4 = 0$. The solution of eq. (2.18) is thus given by

$$H^{(1)}(x^+,x^-,z) = H^{(1)}_0(x^+,x^-)z^4 + H^{(1)}_1(x^+,x^-)z^6 + H^{(1)}_2(x^+,x^-)z^8 + H^{(1)}_3(x^+,x^-)z^{10} \tag{2.22}$$

with the coefficients

$$H^{(1)}_0 = -\frac{6}{(\partial_+\,\partial_-)^2}\,\psi_7 - \frac{96}{(\partial_+\,\partial_-)^3}\,\psi_9 - \frac{2880}{(\partial_+\,\partial_-)^4}\,\psi_{11} \tag{2.23a}$$

JHEP05(2009)060

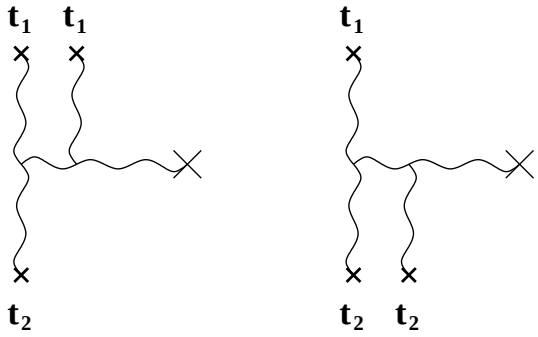

Figure 4. Graviton diagrams corresponding to the NLO solution of Einstein equations found in this section.

$$H_1^{(1)} = -\frac{1}{\partial_+ \partial_-}\,\psi_7 - \frac{16}{(\partial_+ \partial_-)^2}\,\psi_9 - \frac{480}{(\partial_+ \partial_-)^3}\,\psi_{11} \tag{2.23b}$$

$$H_2^{(1)} = -\frac{1}{\partial_+ \partial_-}\,\psi_9 - \frac{30}{(\partial_+ \partial_-)^2}\,\psi_{11} \tag{2.23c}$$

$$H_3^{(1)} = -\frac{1}{\partial_+ \partial_-}\,\psi_{11}. \tag{2.23d}$$

Using $H^{(1)}$ from eq. (2.22) in eq. (2.17a) one can easily find $G^{(1)}$. With the help of two other components of Einstein equations which are not shown here explicitly we can find (and have found) $F^{(1)}$ and $\tilde{F}^{(1)}$. The remaining components of Einstein equations do not generate further constraints.

Note that $G^{(1)}$, $F^{(1)}$ and $\tilde{F}^{(1)}$ are indeed needed to construct the metric at higher orders in the expansion in t's. However, as we argued above and as shown in eq. (2.12), only $H_0^{(1)}$ is needed to obtain the energy-momentum tensor of the produced matter at NLO. Since at NLO $G^{(1)}$, $F^{(1)}$ and $\tilde{F}^{(1)}$ are not needed for the boundary theory physics that we are interested in here, we will not present explicit expressions for these quantities.

The NLO solution in eqs. (2.22) and (2.23) is represented diagrammatically in terms of graviton exchanges in figure 4. As shown in figure 4 the NLO solution consists of a single rescattering in one nucleus and a double rescattering in another nucleus. As can be seen from eqs. (2.23) and (2.19), NLO solution includes terms with two powers of t_1 and one power of t_2 and terms with two powers of t_2 and one power of t_1.

2.2.2 Delta-function shock waves at NLO

It is instructive to find what the obtained results give for specific shock waves described by particular forms of $t_1(x^-)$ and $t_2(x^+)$. Define the transverse pressure p of the produced medium by

$$\langle T^{i\,j} \rangle = \delta^{ij}\, p. \tag{2.24}$$

Combining eq. (2.24) with eqs. (2.12) and (2.14) yields

$$p(x^+, x^-) \;=\; \frac{N_c^2}{2\,\pi^2}\,\left[H_0^{(0)}(x^+, x^-) + H_0^{(1)}(x^+, x^-) + H_0^{(2)}(x^+, x^-) + \cdots\right]. \tag{2.25}$$

JHEP05(2009)060

Let us for simplicity concentrate on this component of the energy-momentum tensor: all others can be also easily constructed using eq. (2.12).

Following the original suggestion of [51] (see also [12]) let us first consider delta-function shock waves

$$t_1(x^-) = \mu_1 \, \delta(x^-), \quad t_2(x^+) = \mu_2 \, \delta(x^+). \tag{2.26}$$

As was argued in [1], the delta-function shock waves give a solution of Einstein equations having correct qualitative features of the solution for any colliding shock waves with non-negative t_1 and t_2. However, plugging the delta-functions from (2.26) into eq. (2.16) and then into eq. (2.19) we immediately encounter a problem: we obtain products of delta-functions and theta functions, like $\delta(x^+)\,\theta(x^+)$. To properly handle those terms let us regulate the delta-functions by spearing them along the light cone directions:

$$t_1(x^-) = \frac{\mu_1}{a_1} \, \theta(x^-) \, \theta(a_1 - x^-), \quad t_2(x^+) = \frac{\mu_2}{a_2} \, \theta(x^+) \, \theta(a_2 - x^+). \tag{2.27}$$

To be more specific let us consider in the boundary theory a collision of two ultrarelativistic nuclei with large light-cone momenta per nucleon p_1^+, p_2^-, and atomic numbers A_1 and A_2. In order to avoid N_c^2 suppression in each graviton exchange coming from the Newton's constant (see e.g. eq. (2.3)) let us assume that each nucleon in the nucleus has N_c^2 nucleons in it. This factor of N_c^2 in $\langle T_{1--} \rangle$ and $\langle T_{2++} \rangle$ cancels the factor of $1/N_c^2$ in eqs. (2.3) and (2.4). In the end one obtains, similar to [1, 73]

$$\mu_1 \sim p_1^+ \, \Lambda_1^2 \, A_1^{1/3}, \quad \mu_2 \sim p_2^- \, \Lambda_2^2 \, A_2^{1/3}, \tag{2.28}$$

while the Lorentz-contracted widths of the nuclei are

$$a_1 \sim \frac{A_1^{1/3}}{p_1^+}, \quad a_2 \sim \frac{A_2^{1/3}}{p_2^-}. \tag{2.29}$$

The scales Λ_1 and Λ_2 are the typical transverse momentum scales describing the two nuclei [1], similar to the saturation scales.

Using eq. (2.27) along with eqs. (2.25), (2.15), (2.16), (2.22), and (2.23a), we obtain

$$p(x^+, x^-) = \frac{N_c^2}{2\pi^2} 8 \mu_1 \mu_2 x^+ x^- \theta(x^+) \theta(x^-) \left[1 - 12 \mu_1 x^+ (x^-)^2 - 12 \mu_2 (x^+)^2 x^- + \cdots \right]. \tag{2.30}$$

In arriving at eq. (2.30) we neglected terms suppressed by powers of a_1/x^- and a_2/x^+. Thus eq. (2.30) is only valid when

$$\frac{a_1}{x^-} \ll 1, \quad \frac{a_2}{x^+} \ll 1. \tag{2.31}$$

However this is not the only constraint on applicability of eq. (2.30): requiring that $o(a_1/x^-, a_2/x^+)$ corrections to the NLO terms are much smaller than LO terms, employing eqs. (2.28) and (2.29), and assuming for simplicity that $p_1^+ \sim p_2^-$, $\Lambda_1 \approx \Lambda_2 \equiv \Lambda$, $A_1 \approx A_2 \equiv A$, we obtain another restriction

$$\Lambda \, A^{1/3} \, \tau \ll 1 \tag{2.32}$$

JHEP05(2009)060

with the proper time $\tau = \sqrt{2\,x^+\,x^-}$. Hence eq. (2.30) is valid at relatively early proper times and acquires order-1 corrections at later times. Indeed eq. (2.30) provides an exact solution in the formal limit of $a_1, a_2 \to 0$ which reduces t_1 and t_2 back to the delta-function expressions given in eq. (2.26). However, eqs. (2.28) and (2.29) demonstrate that if we keep track of the physical origin of the delta-functions, the infinitely-thin nucleus limit gets more involved. Of course one can always postulate the nuclei to be very thin in the longitudinal direction while keeping their atomic numbers fixed, thus making the formal $a_1, a_2 \to 0$ limit possible: such limit is not attainable in real life, but it is a mathematically well-defined procedure.

Eq. (2.30) agrees with the appropriate result obtained in [12] for delta-function shock waves.

2.2.3 Delta-prime shock waves at NLO

In [1] it was argued that delta-function shock waves considered in section 2.2.2 come to a complete stop shortly after the collision, possibly leading to a formation of a black hole. For the boundary theory this implied that the colliding nuclei stop after the collision and thermalize leading to Landau-like hydrodynamics [57]. This scenario would lead to strong baryon stopping in the collisions, which is not what is observed by the experiments at RHIC. Combined with the many successes of small-coupling based approaches in describing RHIC data sensitive to early-time dynamics (for a review see [50]), this led us to conclude that one can not adequately describe entire heavy ion collision within a strong coupling framework. Thus collisions of delta-function shock waves in AdS_5 are not relevant for the heavy ion collisions, in which it is very likely that the initial stages of the collisions are weakly-coupled. In [1] to try to mimic these weak coupling effects we suggested using unphysical delta-prime shock waves

$$t_1(x^-) \,=\, \Lambda_1^2\, A_1^{1/3}\, \delta'(x^-), \quad t_2(x^+) \,=\, \Lambda_2^2\, A_2^{1/3}\, \delta'(x^+). \tag{2.33}$$

The shock waves in eq. (2.33) are fundamentally different from those in section 2.2.2 as the integrals of these shock wave profiles over all x^-'s and/or x^+'s give zero. The shock waves (2.33) have unphysical energy-density on the light cone. However, in the LO calculations carried out in [1] it was shown that the behavior of the produced matter in the forward light cone of a collision of two shock waves (2.33) gives a well-behaved physical distribution of matter. This should be contrasted with the physical shock waves in section 2.2.2, for which, due to nuclear stopping, the remnants of the colliding nuclei would deviate from their initial light cone trajectories and drift into the forward light cone.

To use the shock waves of eq. (2.33) for calculating the NLO contribution to the transverse pressure p we have to regulate them. We do that by rewriting (2.33) as [35, 38]

$$\begin{aligned} t_1(x^-) \,&=\, \Lambda_1^2 \sum_{i=1}^{A_1^{1/3}} \delta'(x^- - x_i^-) \\ t_2(x^+) \,&=\, \Lambda_2^2 \sum_{i=1}^{A_2^{1/3}} \delta'(x^+ - x_i^+). \end{aligned} \tag{2.34}$$

Each delta-prime in eq. (2.34) corresponds to a thin slice of a shock wave (a "nucleon") localized around the longitudinal coordinate $x_i^{\pm}$. The coordinates x_i^- are localized to the interval $[0, a_1]$ of the x^- axis, while the coordinate x_i^+ are localized to the interval $[0, a_2]$ of the x^+ axis.

Employing eq. (2.34) in eqs. (2.25), (2.15), (2.16), (2.22), and (2.23a), and assuming that $A_1, A_2 \gg 1$, yields the transverse pressure

$$p(x^+, x^-) = \frac{N_c^2}{2\pi^2} 8 \Lambda_1^2 A_1^{1/3} \Lambda_2^2 A_2^{1/3} \theta(x^+) \theta(x^-) \left\{ 1 - 40 \left[\Lambda_1^2 A_1^{1/3} + \Lambda_2^2 A_2^{1/3} \right] x^+ x^- \right. \\ \left. -36 \left[\Lambda_1^2 A_1^{1/3} p_1^+ x^+ (x^-)^2 + \Lambda_2^2 A_2^{1/3} p_2^- (x^+)^2 x^- \right] + \dots \right\}. \tag{2.35}$$

Eq. (2.35) is derived in appendix A. Just like with eq. (2.30), in arriving at eq. (2.35) we have neglected terms suppressed by additional powers of energy, i.e., we assumed the condition (2.31) to be valid. At the same time we did not have to assume that the bound (2.32) applies.

From eq. (2.35) we see that NLO corrections in the transverse pressure are of two types: they can be rapidity/energy-independent, like the second term in the square brackets, which is proportional to $x^+ x^- \sim \tau^2$. They can also be rapidity/energy-dependent, like the last term in the square brackets in eq. (2.35), which is proportional to, say, $(x^+)^2 x^- \sim \tau^3 e^\eta$, where we defined the space-time rapidity $\eta = (1/2) \ln(x^+/x^-)$. That term also includes explicit powers of the large momentum components p_1^+ and p_2^-, i.e., it is explicitly energy-dependent. Indeed if $p_1^+ x^- \gg 1$ or $p_2^- x^+ \gg 1$ the last term in the square brackets of eq. (2.35) dominates over the second term in the brackets.

2.3 NNLO results

Evaluation of the NNLO terms goes along the same lines as the NLO calculation. One plugs the expansion of eq. (2.14) into Einstein equations (2.5) and expands the resulting equations up to the quadric order in t's. In particular one obtains the following equations for $G^{(2)}$ and $H^{(2)}$

$$(\perp\perp) \qquad G_z^{(2)} + 5 H_z^{(2)} - z H_{zz}^{(2)} + 2 z H_{x^+ x^-}^{(2)} + \Delta_7 z^7 + \Delta_9 z^9 + \Delta_{11} z^{11} + \\ + \Delta_{13} z^{14} + \Delta_{15} z^{15} = 0 \tag{2.36a}$$

$$(zz) \qquad G_z^{(2)} + 2 H_z^{(2)} - z G_{zz}^{(2)} - 2 z H_{zz}^{(2)} + 48 A_7 z^7 + 80 A_9 z^9 + 120 A_{11} z^{11} + \\ + 168 A_{13} z^{13} + + 224 A_{15} z^{15} = 0 \tag{2.36b}$$

with Δ's and A's being some known functions of t_1 and t_2. Eliminating $G^{(2)}$ from eqs. (2.36a) and (2.36b) yields

$$-3 H_z^{(2)} + 3 z H_{zz}^{(2)} - z^2 H_{zzz}^{(2)} + 2 z^2 H_{x^+ x^- z}^{(2)} + 12 \Psi_7 z^7 + 16 \Psi_9 z^9 + \\ + 20 \Psi_{11} z^{11} + 24 \Psi_{13} z^{13} + 28 \Psi_{15} z^{15} = 0 \tag{2.37}$$

with

$$\Psi_7 = \frac{4}{3} \left[4 h_0^2 - \lambda_1 \lambda_2 + t_1 \frac{\partial_+}{\partial_-} H_0^{(1)} + t_2 \frac{\partial_-}{\partial_+} H_0^{(1)} \right] \tag{2.38a}$$

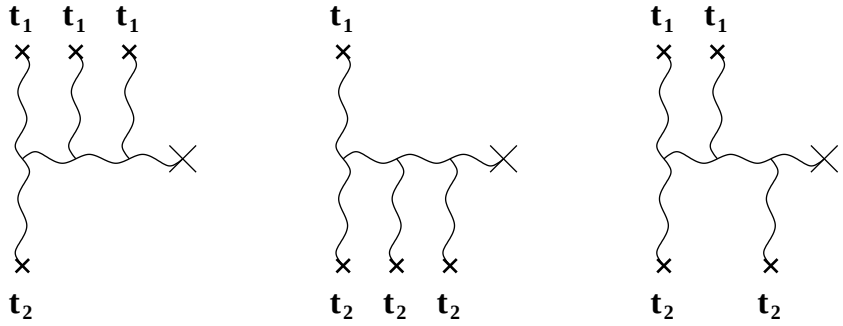

Figure 5. Some of the graviton diagrams corresponding to the NNLO solution of Einstein equations found in section 2.3.

$$\Psi_9 = \frac{1}{4}\Big[-4\,h_{0x^-}\,h_{0x^+} + 16\,h_0\,h_{0\,x^+\,x^-} + \Big\{3\,(-\lambda_2\,h_{0\,x^-\,x^-} + t_2\,H^{(1)}_{0\,x^-\,x^-}) + (x^+ \leftrightarrow x^-;\, 1 \leftrightarrow 2)\Big\}\Big] \tag{2.38b}$$

$$\Psi_{11} = \frac{1}{60}\Big[128\,h_0\,t_1\,t_2 + 34\,(h_{0\,x^+\,x^-})^2 - 13\,h_{0\,x^+\,x^+}\,h_{0\,x^-\,x^-} + \Big\{36 t_2 H^{(1)}_{1x^-x^-} - 10 h_{0x^+} h_{0x^+x^-x^-} - 6\lambda_2 h_{0x^+x^-x^-x^-} + (x^+ \leftrightarrow x^-; 1 \leftrightarrow 2)\Big\}\Big] \tag{2.38c}$$

$$\Psi_{13} = \frac{1}{576}\Big[768\,t_1\,t_2\,h_{0\,x^+\,x^-} - 16\,h_{0\,x^+\,x^-\,x^-}\,h_{0\,x^+\,x^+\,x^-} + \Big\{136\,t_1\,t_2'\,h_{0\,x^-} + 320\,t_2\,H^{(1)}_{2\,x^-\,x^-} - 13\,h_{0\,x^+\,x^-\,x^-\,x^-}\,h_{0\,x^+\,x^+} + (x^+ \leftrightarrow x^-;\, 1 \leftrightarrow 2)\Big\}\Big] \tag{2.38d}$$

$$\Psi_{15} = \frac{1}{504}\Big[368\,t_1^2\,t_2^2 - h_{0\,x^+\,x^-\,x^-\,x^-}\,h_{0\,x^+\,x^+\,x^+\,x^-} + \Big\{270\,t_2\,H^{(1)}_{3\,x^-\,x^-} + 19\,t_1\,t_2'\,h_{0\,x^+\,x^-\,x^-} + (x^+ \leftrightarrow x^-;\, 1 \leftrightarrow 2)\Big\}\Big]. \tag{2.38e}$$

The prime in $t_1'(x^-)$ and in $t_2'(x^+)$ indicates derivatives with respect to the only argument of the functions.

To find a causal solution of eq. (2.37) one expands $H^{(2)}$ into a series in z^2, matches the coefficients of the powers of z^2 and requires the series to terminate at some finite order to find the coefficients. The answer then reads

$$H^{(2)}(x^+,x^-,z) = H_0^{(2)}(x^+,x^-)\,z^4 + H_1^{(2)}(x^+,x^-)\,z^6 + H_2^{(2)}(x^+,x^-)\,z^8 + H_3^{(2)}(x^+,x^-)\,z^{10} + H_4^{(2)}(x^+,x^-)\,z^{12} + H_5^{(2)}(x^+,x^-)\,z^{14} \tag{2.39}$$

with

$$H_0^{(2)} = \frac{6}{\partial_+\,\partial_-}\,H_1^{(2)} \tag{2.40a}$$

$$H_1^{(2)} = -\frac{1}{\partial_+\,\partial_-}\,\psi_7 - \frac{16}{(\partial_+\,\partial_-)^2}\,\Psi_9 - \frac{(16)(30)}{(\partial_+\,\partial_-)^3}\,\Psi_{11} - \frac{(16)(30)(48)}{(\partial_+\,\partial_-)^4}\,\Psi_{13} - \frac{(16)(30)(48)(70)}{(\partial_+\,\partial_-)^5}\,\Psi_{15} \tag{2.40b}$$

$$H_2^{(2)} = -\frac{1}{(\partial_+\,\partial_-)}\,\Psi_9 - \frac{30}{(\partial_+\,\partial_-)^2}\,\Psi_{11} - \frac{(30)(48)}{(\partial_+\,\partial_-)^3}\,\Psi_{13} - \frac{(30)(48)(70)}{(\partial_+\,\partial_-)^4}\,\Psi_{15} \tag{2.40c}$$

JHEP05(2009)060

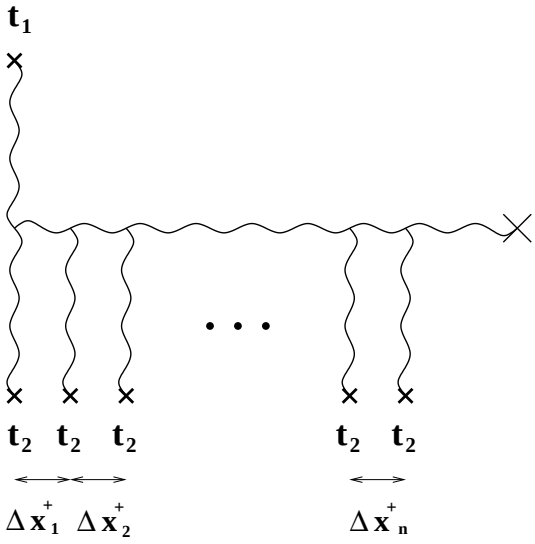

Figure 6. A diagram contributing to the metric of an asymmetric collision of two shock waves as considered in section 3.

$$H_3^{(2)} = -\frac{1}{(\partial_+\,\partial_-)}\,\Psi_{11} - \frac{48}{(\partial_+\,\partial_-)^2}\,\Psi_{13} - \frac{(48)(70)}{(\partial_+\partial_-)^3}\,\Psi_{15} \tag{2.40d}$$

$$H_4^{(2)} = -\frac{1}{(\partial_+\,\partial_-)}\,\Psi_{13} - \frac{70}{(\partial_+\,\partial_-)^2}\,\Psi_{15} \tag{2.40e}$$

$$H_5^{(2)} = -\frac{1}{(\partial_+\,\partial_-)}\,\Psi_{15}. \tag{2.40f}$$

Using eqs. (2.39) with (2.40) in the remaining Einstein equations allows one to find the other components of the metric at the same order: $G^{(2)}$, $F^{(2)}$, and $\tilde{F}^{(2)}$. The essential classes of diagrams resummed at NNLO are shown in figure 5. They involve either three rescatterings in one nucleus and one rescattering in the other nucleus or two rescatterings in each of the nuclei.

3 Asymmetric collisions of shock waves in AdS_5

3.1 Derivation of the equations

We now want to find the solution of the proton-nucleus scattering problem at strong coupling. In other words we want to resum all-order graviton exchanges with one shock wave while keeping only terms with a single graviton exchange with the second nucleus. That is, we want to resum all powers of, say, t_2, while keeping only the leading power of t_1. An example of a typical diagram which is resummed this way is shown in figure 6.

To resum the diagrams of the type shown in figure 6 let us first construct the corresponding Einstein equations describing this classical graviton field. We start by writing the metric, which is just the same as given in eq. (2.7), but without capitalizing the unknown

JHEP05(2009)060

functions, to distinguish from the case of the full nucleus-nucleus collisions:

$$ds^2 = \frac{L^2}{z^2}\Big\{ -\big[2+g(x^+,x^-,z)\big]\,dx^+\,dx^- + \big[t_1(x^-)\,z^4 + f(x^+,x^-,z)\big]\,dx^{-\,2} + \Big[t_2(x^+)\,z^4 + \tilde{f}(x^+,x^-,z)\Big]\,dx^{+\,2} + [1+h](x^+,x^-,z)\,dx_\perp^2 + dz^2\Big\}. \tag{3.1}$$

We now want to plug the metric (3.1) into the Einstein equations (2.5) and linearize it in t_1. In doing so we have to remember that, as f, $\tilde{f}$, g, and h should have only one factor of t_1 in them, one has $f, \tilde{f}, g, h \sim t_1$. Thus one has to linearize Einstein equations in t_1 and in f, $\tilde{f}$, g and h. The relevant equations are

$$(\perp\perp) \quad -4\,z^3\,t_2\,f - 8\,z^7\,t_1\,t_2 - z^4\,t_2\,f_z + g_z + 5\,h_z - z\,h_{z\,z} + z^5\,t_2\,h_{x^-\,x^-} + 2\,z\,h_{x^+\,x^-} = 0 \tag{3.2a}$$

$$(zz) \quad 8\,z^3\,t_2\,f + 32\,z^7\,t_1\,t_2 + 3\,z^4\,t_2\,f_z + g_z + 2\,h_z + z^5\,t_2\,f_{z\,z} - z\,g_{z\,z} - 2\,z\,h_{z\,z} = 0 \tag{3.2b}$$

$$(-z) \quad z^7\,t_1'\,t_2 + z^3\,t_2\,f_{x^-} - \frac{1}{4}\,g_{x^-\,z} - h_{x^-\,z} - \frac{1}{2}\,f_{x^+\,z} = 0, \tag{3.2c}$$

where we suppressed the arguments of all functions and, as usual, the subscripts z, x^+ and x^- indicate partial derivatives with respect to these variables. Again, the prime in $t_1'(x^-)$ (and in $t_2'(x^+)$ below) indicates a derivative with respect to the only argument of the function. Other components of Einstein equations are not needed, as eqs. (3.2) contain enough information to find f, g and h. In fact we will need to know only h: as was shown in eqs. (2.12) we can reconstruct the whole energy-momentum tensor of the produced matter from it.

Solving eq. (3.2a) for g_z and using the result to eliminate g from eq. (3.2c) yields

$$\frac{1}{4}\,h_z - \frac{1}{2}\,\frac{\partial_+}{\partial_-}\,f_z - \frac{1}{4}\,z\,\big[h_{z\,z} + z^3\,t_2\,(4\,z^3\,t_1 + f_z - z\,h_{x^-\,x^-}) - 2\,h_{x^+\,x^-}\big] = 0. \tag{3.3}$$

Eliminating g_z from eq. (3.2b) and solving the resulting equation for f_z we get

$$f_z = \frac{1}{4\,z^4\,t_2}\,\big[-16\,z^7\,t_1\,t_2 - 3\,h_z + 3\,z\,h_{z\,z} - z^2\,h_{z\,z\,z} + 4\,z^5\,t_2\,h_{x^-\,x^-} + z^6\,t_2\,h_{x^-\,x^-\,z} + 2\,z^2\,h_{x^+\,x^-\,z}\big]. \tag{3.4}$$

Applying an operator ∂_-/∂_+ to eq. (3.3) and substituting f_z from eq. (3.4) into it we obtain the following equation for h

$$-3\,h_z + 3\,z\,h_{z\,z} - z^2\,h_{z\,z\,z} + 2\,z^2\,h_{x^+\,x^-\,z} = 16\,z^7\,t_1\,t_2 + z^4\,t_2\,\frac{\partial_-}{\partial_+}\left[\frac{7}{2}\,h_z - \frac{7}{2}\,z\,h_{z\,z} + \frac{1}{2}\,z^2\,h_{z\,z\,z} - 2\,z^2\,h_{x^+\,x^-\,z} - \frac{1}{2}\,z^6\,t_2\,h_{x^-\,x^-\,z}\right]. \tag{3.5}$$

Note that the first line of eq. (3.5) is identical to the LO equation (4.10) in [1]. Higher order powers of t_2 come in through the second line of eq. (3.5).

JHEP05(2009)060

Eq. (3.5) is the equation we need to solve. We slightly simplify it by writing it as

$$z^2\,\partial_z\left[\frac{3}{z}\,h_z - h_{z\,z} + 2\,h_{x^+\,x^-}\right] = 16\,z^7\,t_1\,t_2 + z^4\,t_2\,\frac{\partial_-}{\partial_+}\left\{z^2\,\partial_z\left[-\frac{7}{2}\,\frac{1}{z}\,h_z + \frac{1}{2}\,h_{z\,z} - 2\,h_{x^+\,x^-}\right] - \frac{1}{2}\,z^4\,t_2\,\partial_-^2\,z^2\,\partial_z h\right\}. \quad (3.6)$$

Below we will use eq. (3.6) to evaluate the diagram in figure 6 in the eikonal approximation, which we will define in the next Subsection.

3.2 Green function and the eikonal approximation

To construct the solution of eq. (3.6) we will need to construct the retarded Green function of the operator on its left hand side. As inverting $z^2\,\partial_z$ is trivial, we will need the function $G(x^+, x^-, z; x'^+, x'^-, z')$ such that

$$\left[\frac{3}{z}\partial_z - \partial_z^2 + 2\partial_+\partial_-\right] G(x^+, x^-, z; x'^+, x'^-, z') = \delta(x^+ - x'^+)\delta(x^- - x'^-)\delta(z - z'). \quad (3.7)$$

This is a bulk-to-bulk scalar field propagator, which has previously been found in [74]. For completeness of the presentation let us briefly outline the construction of $G(x^+, x^-, z; x'^+, x'^-, z')$.

Fourier-transforming eq. (3.7) into light-cone momentum space (i.e., going from x^+ and x^- coordinates to their conjugates k^+, k^- but keeping the coordinate z) and dropping the delta-function on the right one can see that the solution of the resulting equation is simply $z^2\,J_2(z\sqrt{2\,k^+\,k^-})$. Using these Bessel function and going back to the x^0, x^3 coordinates instead of x^+, x^- we write for the retarded Green function

$$G(x^0, x^3, z; x'^0, x'^3, z') = \frac{\theta(x^0 - x'^0)}{2\,\pi}\int\limits_0^\infty dm \int\limits_{-\infty}^\infty dk\,\frac{\sin\left[(x^0 - x'^0)\sqrt{m^2 + k^2}\right]}{\sqrt{m^2 + k^2}}\,e^{i\,k\,(x^3 - x'^3)} \times\, m\,z^2\,J_2(m\,z)\,\frac{1}{z'}\,J_2(m\,z'). \quad (3.8)$$

The integral over the momentum variable k can be performed yielding

$$G(x^+, x^-, z; x'^+, x'^-, z') = \frac{1}{2}\,\theta(x^+ - x'^+)\,\theta(x^- - x'^-)\,\frac{z^2}{z'}\int\limits_0^\infty dm \times\, m\,J_0\left(m\,\sqrt{2\,(x^+ - x'^+)\,(x^- - x'^-)}\right)\,J_2(m\,z)\,J_2(m\,z'). \quad (3.9)$$

Eq. (3.9) can be further simplified by integration over m, which gives

$$G(x^+, x^-, z; x'^+, x'^-, z') = \frac{1}{2\pi}\theta(x^+ - x'^+)\theta(x^- - x'^-)\theta(s)\theta(2 - s)\,\frac{z}{z'^2}\,\frac{1 + 2s(s-2)}{\sqrt{s(2-s)}} \quad (3.10)$$

with

$$s \equiv \frac{2\,(x^+ - x'^+)\,(x^- - x'^-) - (z - z')^2}{2\,z\,z'}. \quad (3.11)$$

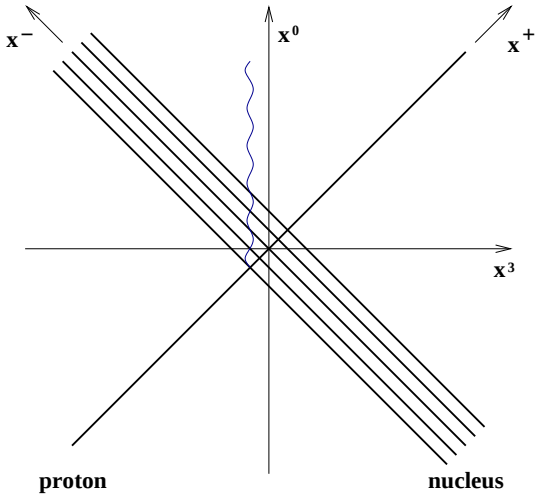

Figure 7. The space-time structure of the graviton emission in a proton-nucleus collision. The graviton is denoted by the wavy line. After being produced the graviton rescatters in the nucleus and the propagates freely in the forward light-cone.

However eq. (3.9) is really all we need for the calculations to follow.

Eqs. (3.9) or (3.10) give us the propagator of the gravitons in the s-channel of figure 6. These expressions allow us to construct the eikonal approximation for the graviton production in asymmetric shock wave collisions. The space-time structure of graviton production in such collisions in shown in figure 7. It illustrates the diagram in figure 6: first the graviton (the wavy line) is produced in a collision of the proton shock wave and some elements of the nucleus shock wave (a nucleon in the nucleus). This generates the LO factor of $t_1\, t_2$. Subsequently the graviton rescatters in the nucleus shock wave with each rescattering bringing in a factor of t_2. After the graviton leaves the shock wave it simply propagates freely. Indeed the transverse dimensions x^1, x^2 and the 5th dimension in AdS_5 are implied but not shown in figure 7.

Most importantly, the propagation of the graviton between two successive rescatterings in the nucleus shock wave happens over a very short interval in the light-cone "plus" direction. Namely the intervals Δx_i^+'s between the rescatterings in figure 6 are Lorentz-contracted and are all of the order $\Delta x_i^+ \sim 1/p_2^-$. As p_2^- (along with the comparable scale p_1^+) is the largest momentum scale in the problem we conclude that Δx_i^+'s are the shortest distance scales in the problem, i.e., they are *very small* compared to any other distance scale. This is illustrated in figure 7, which depicts the propagation of the graviton through the highly Lorentz-contracted nucleus. Therefore we can approximate the full s-channel graviton propagator by its short-x^+-interval version. We will call such approximation an *eikonal approximation* in analogy with the terminology used in high energy scattering in four dimensions.

Putting $x^+ \approx x'^+$ in eq. (3.9) we can put $J_0(0) = 1$ which yields the Green function in

JHEP05(2009)060

the eikonal approximation

$$G_{\rm eik}(x^+,x^-,z;x'^+\approx x^+,x'^-,z') = \frac{1}{2}\theta(x^+-x'^+)\theta(x^--x'^-)\frac{z^2}{z'}\int\limits_0^\infty dm m J_2(mz)J_2(mz')$$
$$= \frac{1}{2}\theta(x^+-x'^+)\theta(x^--x'^-)\delta(z-z'). \qquad (3.12)$$

For inhomogeneous equations like (3.6), or like the following equation

$$\frac{3}{z}\,h_z - h_{z\,z} + 2\,h_{x^+\,x^-} \;=\; R(x^+,x^-,z), \qquad (3.13)$$

in the solution, the Green function acts on some function $R(x^+,x^-,z)$ on the right hand side, such that

$$h(x^+,x^-,z) \;=\; \int\limits_{-\infty}^{\infty} dx'^+ \int\limits_{-\infty}^{\infty} dx'^- \int\limits_0^\infty dz'\, G(x^+,x^-,z;x'^+,x'^-,z')\, R(x'^+,x'^-,z'). \qquad (3.14)$$

Using the eikonal Green function (3.12) in eq. (3.14) yields

$$h_{\rm eik}(x^+,x^-,z) \;=\; \frac{1}{2\,\partial_+\,\partial_-}\,R(x^+,x^-,z) \qquad (3.15)$$

with the inverse derivatives defined in eq. (2.13).

Going from eq. (3.13) to eq. (3.15) clarifies the procedure for the eikonal approximation: simply neglecting all z-derivatives on the left hand side of eq. (3.13) compared to ∂_+ we obtain eq. (3.15). Indeed $\partial_+ \sim 1/\Delta x^+ \sim p_2^-$ if the propagator in question spans a short interval Δx^+. Hence the main rule of the eikonal approximation is that ∂_+ is much larger than any other derivative in the problem. The short interval scalar field bulk-to-bulk propagator is

$$\int\limits_{-\infty}^{\infty} dx'^+ \int\limits_{-\infty}^{\infty} dx'^- \int\limits_0^\infty dz'\, G_{\rm eik}(x^+,x^-,z;x'^+,x'^-,z')\,[\ldots] \;=\; \frac{1}{2\,\partial_+\,\partial_-}\,[\ldots]\,. \qquad (3.16)$$

One has to keep in mind that the eikonal approximation should be applied to short-lived propagators only. That is we can not just take eq. (3.6) and drop all terms not containing ∂_+. As can be seen from figures 6 and 7, the graviton propagator after the interaction with the nucleus is not limited to any short interval in any direction. That is, we have to use the full propagator (3.9) for that line. Note that we are not calculating the graviton production amplitude: we are calculating the graviton field. Hence in the diagram in figure 6 the outgoing graviton propagator is off-mass shell, and is *not* on mass shell, as it would have been for the production amplitude. (See e.g. [36] for an example of constructing Feynman diagrams corresponding to classical fields.)

The graviton propagator in eq. (3.16) does not take into account rescatterings and only describes free propagation for a graviton over a short time interval. The eikonal approximation should also be applied to the multi-graviton vertices in figure 6. To facilitate

JHEP05(2009)060

the application of the eikonal approximation let us recast eq. (3.6) in a slightly different form. Defining

$$\tilde{h} \;=\; z^2\,\partial_z\,h \tag{3.17}$$

we rewrite eq. (3.6) as

$$\left[\hat{D}_1 + 2\,\partial_+\,\partial_-\right]\,\tilde{h} \;=\; 16\,z^7\,t_1\,t_2 + z^4\,t_2\,\frac{\partial_-}{\partial_+}\,\left\{\left[\hat{D}_2 - 2\,\partial_+\,\partial_-\right]\,\tilde{h} - \frac{1}{2}\,z^4\,t_2\,\partial_-^2\,\tilde{h}\right\} \tag{3.18}$$

where we have defined differential operators

$$\hat{D}_1 \;=\; z^2\,\partial_z\,\left[\frac{5}{z^3} - \frac{1}{z^2}\,\partial_z\right] \tag{3.19}$$

and

$$\hat{D}_2 \;=\; z^2\,\partial_z\,\left[-\frac{9}{2}\,\frac{1}{z^3} + \frac{1}{2}\,\frac{1}{z^2}\,\partial_z\right]. \tag{3.20}$$

Defining the truncated amplitude

$$\bar{h} \;=\; \left[\hat{D}_1 + 2\,\partial_+\,\partial_-\right]\,\tilde{h} \tag{3.21}$$

allows us to write eq. (3.18) as

$$\bar{h} = 16z^7t_1t_2 + z^4t_2\frac{\partial_-}{\partial_+}\left[\left(\hat{D}_2 - 2\partial_+\partial_-\right)\left(\hat{D}_1 + 2\partial_+\partial_-\right)^{-1} - \frac{1}{2}z^4t_2\partial_-^2\left(\hat{D}_1 + 2\partial_+\partial_-\right)^{-1}\right]\bar{h}. \tag{3.22}$$

The solution of eq. (3.22) is

$$\bar{h} = \left[1 + z^4t_2\frac{\partial_-}{\partial_+}\left(1 - \frac{\hat{D}_2}{2\partial_+\partial_-}\right)\left(1 + \frac{\hat{D}_1}{2\partial_+\partial_-}\right)^{-1} + \frac{1}{4}\left(z^4t_2\frac{\partial_-}{\partial_+}\right)^2\left(1 + \frac{\hat{D}_1}{2\partial_+\partial_-}\right)^{-1}\right]^{-1} \times 16z^7t_1t_2. \tag{3.23}$$

As t_2 and $1/\partial_+$ do not commute, here and throughout the paper we have

$$\left(t_2\,\frac{1}{\partial_+}\right)^2\,\ldots \;=\; t_2\,\frac{1}{\partial_+}\left(t_2\,\frac{1}{\partial_+}\,\ldots\right), \tag{3.24}$$

that is, each $1/\partial_+$ operator acts on *everything* to its right.

A simple algebra gives

$$h = \left[\frac{3}{z}\,\partial_z - \partial_z^2 + 2\,\partial_+\,\partial_-\right]^{-1}\,\frac{1}{\partial_z}\,\left(\frac{\bar{h}}{z^2}\right) \tag{3.25}$$

with

$$\frac{1}{\partial_z}\,[\ldots](z) \;=\; \int_0^z dz'\,[\ldots](z')\,. \tag{3.26}$$

Therefore h and $\bar{h}$ are related to each other with the help of the Green function (3.9). Therefore $\bar{h}$ is really the part of the amplitude in figure 6 without the last s-channel gluon propagator, i.e., $\bar{h}$ is the truncated amplitude. As all s-channel graviton propagators in the truncated amplitude $\bar{h}$ are short-lived, we can apply the eikonal approximation to the equation (3.23) for $\bar{h}$. In fact eq. (3.23) is already cast in the form designed to simplify the expansion in inverse powers of ∂_+. The eikonal $\bar{h}$ we obtain this way can be used in eq. (3.25) with the full Green function (3.9) to recover $h(x^+, x^-, z)$. As eq. (3.23) appears to be prohibitively complicated to evaluate analytically, the eikonal approximation appears to be the only way to proceed. In fact, as we will shortly see, for the delta-function shock waves it yields the exact solution for the metric generated in the asymmetric (proton-nucleus) collision of two shock waves.

3.3 Delta-function shock waves

3.3.1 Energy-momentum tensor of the produced medium

Let us again consider a collision of two physical delta-function shock waves with t_1 and t_2 given by eq. (2.26). We will also keep the smeared shock waves in eq. (2.27) in mind.

First let us apply the eikonal approximation to eq. (3.23) without substituting the explicit expressions for t_1 and t_2 from eq. (2.26). As we argued above, in the eikonal approximation the derivative ∂_+ is the largest momentum scale in the problem. Hence in eq. (3.23) we have

$$\frac{\hat{D}_1}{2\,\partial_+\,\partial_-} \ll 1, \quad \frac{\hat{D}_2}{2\,\partial_+\,\partial_-} \ll 1. \tag{3.27}$$

After neglecting those terms eq. (3.23) yields

$$\bar{h}_{\text{eik}} = \left[\left(1 + \frac{1}{2}\, z^4\, t_2\, \frac{\partial_-}{\partial_+}\right)^2\right]^{-1} 16\, z^7\, t_1\, t_2. \tag{3.28}$$

To evaluate eq. (3.28) we expand it in a series

$$\bar{h}_{\text{eik}} = \sum_{n=0}^{\infty} (n+1) \left(-\frac{1}{2}\, z^4\, t_2\, \frac{\partial_-}{\partial_+}\right)^n 16\, z^7\, t_1\, t_2. \tag{3.29}$$

Using eq. (3.29) in eq. (3.25) along with eq. (3.9) we write

$$\begin{aligned} h_{\text{eik}} &= \int\limits_{-\infty}^{\infty} dx'^+ \int\limits_{-\infty}^{\infty} dx'^- \int\limits_{0}^{\infty} dz' G(x^+, x^-, z; x'^+, x'^-, z') \frac{1}{\partial_{z'}} \left(\frac{\bar{h}_{\text{eik}}}{z'^2}\right) \\ &= \int\limits_{-\infty}^{x^+} dx'^+ \int\limits_{-\infty}^{x^-} dx'^- \int\limits_{0}^{\infty} dz' \frac{1}{2} \frac{z^2}{z'} \int\limits_{0}^{\infty} dm m J_0\left(m\sqrt{2(x^+ - x'^+)(x^- - x'^-)}\right) J_2(mz) J_2(mz') \\ &\quad \times \sum_{n=0}^{\infty} \frac{n+1}{2n+3} \left(-\frac{1}{2} t_2(x'^+) \frac{\partial'_-}{\partial'_+}\right)^n 8 (z')^{4n+6} t_1(x'^-) t_2(x'^+). \end{aligned} \tag{3.30}$$

JHEP05(2009)060

Here $\partial'_\pm = \partial/\partial x'^\pm$. The expression (3.30) is still rather difficult to evaluate. However, as we are primarily interested in the dynamics of the gauge theory, we only need the z^4 term in this expression to obtain the transverse pressure of the produced medium using eqs. (2.12) and (2.24). As the series expansion of the Bessel functions converges everywhere, we expand

$$J_2(m\,z) = \frac{1}{8}\,m^2\,z^2 + o(z^4) \tag{3.31}$$

in eq. (3.30) and integrate over z' and m obtaining the transverse pressure

$$\begin{aligned} p =& \frac{N_c^2}{2\pi^2} 8 \sum_{n=0}^{\infty} (n+1)^2 (-2)^n \int\limits_{-\infty}^{x^+} dx'^+ \int\limits_{-\infty}^{x^-} dx'^- (x^+ - x'^+)^{1+2n} (x^- - x'^-)^{1+2n} \\ & \times \left[\partial'^n_- t_1(x'^-)\right] \left(t_2(x'^+) \frac{1}{\partial'_+}\right)^n t_2(x'^+). \end{aligned} \tag{3.32}$$

Using integration by parts in the integral over x'^- in eq. (3.32) and remembering that t_1 is a localized function of x^- yields the final expression for the transverse pressure

$$\begin{aligned} p =& \frac{N_c^2}{2\pi^2} 8 \sum_{n=0}^{\infty} (-2)^n (n+1) \frac{(2n+1)!}{n!} \int\limits_{-\infty}^{x^-} dx'^- (x^- - x'^-)^{1+n} t_1(x'^-) \\ & \times \int\limits_{-\infty}^{x^+} dx'^+ (x^+ - x'^+)^{1+2n} \left(t_2(x'^+) \frac{1}{\partial'_+}\right)^n t_2(x'^+). \end{aligned} \tag{3.33}$$

Eq. (3.33) is one of the main results of this section. It is the simplest expression for p we could find without using an explicit form for the functions t_1 and t_2.

As with the NLO calculations of section 2.2.2, substituting t_1 and t_2 from eq. (2.26) into eq. (3.33) would generate terms like $\delta(x^+)\,\theta(x^+)$, evaluation of which is ambiguous. To avoid this ambiguity we use the smeared t_1 and t_2 from eq. (2.27). For $x^- \gg a_1$ and $x^+ \gg a_2$ we have

$$\int\limits_{-\infty}^{x^-} dx'^- \,(x^- - x'^-)^{1+n}\, t_1(x'^-) \;\approx\; \mu_1\,(x^-)^{1+n}\,\theta(x^-) \tag{3.34}$$

and

$$\int\limits_{-\infty}^{x^+} dx'^+ \,(x^+ - x'^+)^{1+2n} \left(t_2(x'^+)\,\frac{1}{\partial'_+}\right)^n t_2(x'^+) \;\approx\; \frac{1}{(n+1)!}\,\mu_2^{n+1}\,(x^+)^{1+2\,n}\,\theta(x^+). \tag{3.35}$$

Using eqs. (3.34) and (3.35) in eq. (3.33) and summing the series over n yields

$$p \;=\; \frac{N_c^2}{2\,\pi^2}\,\frac{8\,\mu_1\,\mu_2\,x^+\,x^-\,\theta(x^+)\,\theta(x^-)}{[1 + 8\,\mu_2\,(x^+)^2\,x^-]^{3/2}}. \tag{3.36}$$

This is another main result of this section: eq. (3.36) gives us the transverse pressure of the medium produced in the collision of a proton and a nucleus at strong coupling. It is valid at $x^- \gg a_1$ and $x^+ \gg a_2$: these conditions are automatically satisfied if the sources are exact delta-functions of eq. (2.26). Hence for the delta-function sources (2.26) eq. (3.36) provides us with the exact solution of the problem! As a cross-check one can see that expanding eq. (3.36) in a series in μ_2 to NLO yields eq. (2.30).

Eq. (3.36) allows us to explicitly specify the limits of our approximation. Namely, we resum all powers of rescattering in the nucleus, which, for delta-function shock waves translate into powers of $\mu_2 (x^+)^2 x^-$. At the same time we neglect higher rescatterings in the proton, which, by analogy, would bring in powers of $\mu_1 (x^-)^2 x^+$. Hence the applicability region of eq. (3.36) is defined by

$$\mu_1 (x^-)^2 x^+ \ll 1, \quad \mu_2 (x^+)^2 x^- \sim 1. \tag{3.37}$$

(Indeed for small $\mu_2 (x^+)^2 x^-$ eq. (3.36) applies too.) For non-delta function shock waves like those given in eq. (2.27) one also has to keep the limit (2.32) in mind while studying the applicability region of eq. (3.36).

Using eq. (3.36) along with eq. (2.12) we can find all other non-zero components of the energy-momentum tensor of the produced medium:

$$\langle T^{++} \rangle = - \frac{N_c^2}{2\pi^2} \frac{4\mu_1\mu_2 (x^+)^2 \theta(x^+)\theta(x^-)}{[1+8\mu_2 (x^+)^2 x^-]^{3/2}}, \tag{3.38a}$$

$$\langle T^{--} \rangle = \frac{N_c^2}{2\pi^2} \theta(x^+)\theta(x^-) \frac{\mu_1}{2\mu_2 (x^+)^4} \times \frac{3-3\sqrt{1+8\mu_2 (x^+)^2 x^-}+4\mu_2 (x^+)^2 x^- \left(9+16\mu_2 (x^+)^2 x^- -6\sqrt{1+8\mu_2 (x^+)^2 x^-}\right)}{[1+8\mu_2 (x^+)^2 x^-]^{3/2}}, \tag{3.38b}$$

$$\langle T^{+-} \rangle = \frac{N_c^2}{2\pi^2} \frac{8\mu_1\mu_2 x^+ x^- \theta(x^+)\theta(x^-)}{[1+8\mu_2 (x^+)^2 x^-]^{3/2}}, \tag{3.38c}$$

$$\langle T^{ij} \rangle = \delta^{ij} \frac{N_c^2}{2\pi^2} \frac{8\mu_1\mu_2 x^+ x^- \theta(x^+)\theta(x^-)}{[1+8\mu_2 (x^+)^2 x^-]^{3/2}}. \tag{3.38d}$$

Provided the complexity of the problem at hand, the resulting formulas (3.38) for the energy-momentum tensor are remarkably simple!

Now we can ask a question: what kind of medium is produced in these strongly coupled proton-nucleus collisions? Is it described by ideal hydrodynamics, just like Bjorken hydrodynamics was obtained in [51]? In our case the produced matter distribution is obviously rapidity-dependent, so it is slightly more tricky to check whether eqs. (3.38) constitute an ideal hydrodynamics, i.e., whether it can be written as

$$T^{\mu\nu} = (\epsilon + p)\, u^\mu\, u^\nu - p\, \eta^{\mu\nu} \tag{3.39}$$

with the positive energy density ϵ and pressure p. $\eta^{\mu\nu}$ is the metric of the four-dimensional Minkowski space-time and u^μ is the fluid 4-velocity.

JHEP05(2009)060

For the particular case at hand it is easy to see that the energy-momentum tensor in eq. (3.38) can not be cast in the ideal hydrodynamics form of (3.39). In the case of ideal hydrodynamics one has

$$T^{++} \,=\, (\epsilon + p)\,(u^+)^2 \,>\, 0. \tag{3.40}$$

At the same time $\langle T^{++}\rangle$ in eq. (3.38a) is *negative definite*. Therefore the ideal hydrodynamic description is not achieved in the proton-nucleus collisions. We believe this result is due to limitations of this proton-nucleus approximation. Any strongly coupled medium at asymptotically late times is almost certainly bound to thermalize. Our conclusion is then that thermalization/isotropization of the medium does not happen in the space-time region defined by the bounds in eq. (3.37). What we found in eq. (3.38) is a medium at some intermediate stage, presumably on its way to thermalization at a later time. It is likely that one needs to solve the full nucleus-nucleus scattering problem to all orders, as shown in figure 2, to obtain a medium described by ideal hydrodynamics.

3.3.2 Proton stopping

In [1] it was argued that the physical shock waves given by eq. (2.26) or by eq. (2.27) come to a complete stop shortly after the collision. The conclusion was based on the LO calculation, which for the shock waves (2.27) gave the following ++ component of the energy momentum tensor of a nucleus (or its remnants) moving in the light-cone plus direction after the collision

$$\langle T^{++}(x^+ \gg a, x^- = a/2)\rangle \,=\, \frac{N_c^2}{2\,\pi^2}\,\frac{\mu}{a}\,\left[1 - 2\,\mu\,{x^+}^2\,a\right]. \tag{3.41}$$

In arriving at eq. (3.41) in [1] we for simplicity put $\mu_1 = \mu_2 = \mu$ and $a_1 = a_2 = a$. Eq. (3.41) allowed us to conclude that as the light-cone time $x^+ \sim 1/\sqrt{\mu\,a}$ the ++ component of the energy momentum tensor of the shock wave would become zero, meaning that the shock wave stops propagating along the light cone. Indeed, as we saw above (see eq. (3.37)), at the same time as the stopping happens, i.e., when $\mu\,{x^+}^2\,a \sim 1$, higher order graviton exchanges would become important. With the help of eq. (3.33) we can now explore whether multiple graviton exchanges with the nucleus shock wave modify our conclusion about proton stopping reached in [1] at the LO level.

We start by evaluating eq. (3.33) for $x^+ \gg a_2$, but with $0 < x^- < a_1$. That way we follow the proton shock wave for some time after the collision, which allows us to find the energy-momentum tensor of the shock wave itself. As $x^+ \gg a_2$ still, eq. (3.35) remains unchanged. We have to re-evaluate the left-hand-side of eq. (3.34) for $0 < x^- < a_1$. This can be readily done yielding

$$\int\limits_{-\infty}^{x^-} dx'^-\,(x^- - x'^-)^{1+n}\,t_1(x'^-) \,=\, \frac{\mu_1}{a_1}\,\frac{1}{n+2}\,(x^-)^{2+n}, \quad \text{for} \quad 0 < x^- < a_1. \tag{3.42}$$

Using eqs. (3.35) and (3.42) in eq. (3.33) and resumming the series one obtains the transverse pressure inside the proton shock wave, which, with the help of eq. (2.12), gives

the following expression for the ++ component of the energy momentum tensor of the produced matter

$$\langle T^{++}_{\rm prod}\rangle \,=\, \frac{N_c^2}{2\,\pi^2}\,\frac{\mu_1}{a_1}\,\left\{-1+\frac{1}{\sqrt{1+8\,\mu_2\,(x^+)^2\,x^-}}\right\},\quad \text{for}\quad 0<x^-<a_1. \tag{3.43}$$

Eqs. (2.3) and (2.27) give the energy-momentum tensor of the original incoming shock wave itself as

$$\langle T^{++}_{\rm orig}\rangle \,=\, \frac{N_c^2}{2\,\pi^2}\,\frac{\mu_1}{a_1},\quad \text{for}\quad 0<x^-<a_1. \tag{3.44}$$

Adding the energy-momentum tensors of the original shock wave and the produced matter given in eqs. (3.44) and (3.43) together we obtain the total ++ component of the energy-momentum tensor of the proton shock wave

$$\langle T^{++}_{\rm tot}\rangle \,=\, \langle T^{++}_{\rm orig}\rangle + \langle T^{++}_{\rm prod}\rangle \,=\, \frac{N_c^2}{2\,\pi^2}\,\frac{\mu_1}{a_1}\,\frac{1}{\sqrt{1+8\,\mu_2\,(x^+)^2\,x^-}},\quad \text{for}\quad 0<x^-<a_1. \tag{3.45}$$

Expanding eq. (3.45) in the powers of μ_2 at $x^- = a_1/2$ would yield eq. (3.41), providing an independent consistency check.

Eq. (3.45) clearly demonstrates that the ++ component of the energy-momentum tensor of the proton shock wave is *positive definite*. Notice that the LO solution (3.41) for T^{++} becomes negative at large enough x^+. Inclusion of multiple graviton exchanges fixes this problem. T^{++} in eq. (3.45) goes to zero smoothly as x^+ grows large for any fixed x^- in the $0 < x^- < a_1$ range. Thus eq. (3.45) explicitly demonstrates that strong-coupling interactions of the proton shock wave with the nucleus shock wave would stop the proton shock wave shortly after the collision. For $x^- = a_1/2$ the stopping happens at $x^+ \sim 1/\sqrt{\mu_2\,a_1}$, in agreement with the arguments of [1].

3.4 Delta-prime shock waves

3.4.1 Deltology

The eikonal approximation used in section 3.3 reduces the exact formula (3.23) to eq. (3.28). Eq. (3.28) resums the powers of t_2 with only one factor of $1/\partial_+$ inserted between each pair of t_2's. It thus resums terms consisting of sequences like

$$t_2\,\frac{1}{\partial_+}\,t_2\,\frac{1}{\partial_+}\,t_2\,\frac{1}{\partial_+}\,\ldots\,\frac{1}{\partial_+}\,t_2 \tag{3.46}$$

(see also eq. (3.33)). This is indeed natural in the eikonal approximation, as $\partial_+ \sim p_2^-$ is large and we want to have as little powers of $1/\partial_+ \sim 1/p_2^-$ as possible in each term. Eq. (3.28) resums the absolute minimum number of the powers of $1/\partial_+$.

An attentive reader might have noticed that the approximation of eq. (3.28) is insufficient for the delta-prime shock waves of eq. (2.33). Indeed performing the calculation in appendix A we saw that leading powers of p_2^- arose not only from the terms of the type shown in eq. (3.46), like we had in eq. (A.10), but also from terms with two powers

JHEP05(2009)060

of $1/\partial_+$ inserted between two t_2's, as can be seen from eqs. (A.6) and (A.9). Hence we need to rethink our power counting if we want to resum the leading eikonal terms for the delta-prime shock waves.

Let us start with delta-function shock waves with $t_2 \sim \delta(x^+)$. In this case

$$t_2 \frac{1}{\partial_+} t_2 \sim \delta(x^+)\,\theta(x^+) \sim \delta(x^+). \tag{3.47}$$

Here we are being rather sloppy in treating $\delta(x^+)\,\theta(x^+)$: of course the whole regularization introduced in eq. (2.27) above was designed to obtain the correct values for $\theta(0)$ in different situations. However, for the purposes of counting powers of p_2^- the exact value of $\theta(0)$ is not important as long as it is a p_2^--independent number. Eq. (3.47) demonstrates that for $t_2 \sim \delta(x^+)$ one has

$$t_2 \frac{1}{\partial_+} t_2 \frac{1}{\partial_+} t_2 \frac{1}{\partial_+} \dots \frac{1}{\partial_+} t_2 \sim \delta(x^+). \tag{3.48}$$

Therefore $t_2\,(1/\partial_+) \sim o(1)$ in p_2^- power counting.

Higher order corrections may come in through an insertion of one power of $1/\partial_+^2$ between two t_2's. One then gets

$$t_2 \frac{1}{\partial_+^2} t_2 \sim \delta(x^+)\,x^+\,\theta(x^+) = 0. \tag{3.49}$$

The equality in eq. (3.49) is only true for delta-function shock waves and demonstrates that eq. (3.38) is the exact solution for the problem of the collision of two delta-function shock waves. For the smeared shock waves of eq. (2.27) the zero in eq. (3.49) would be replaces by $a_2\,\delta(x^+)$. As $a_2 \sim 1/p_2^-$ this indicates suppression by a power of $1/p_2^-$ compared to the leading-order terms in eq. (3.48). One can similarly show that insertions of higher powers of $1/\partial_+$ would bring in further suppression. Thus our approximation in section 3.3 is justified by this explicit power counting.

Let us now turn our attention to delta-prime shock waves of eq. (2.33). Notice that t_1 and t_2 in eq. (2.33) do not explicitly depend on p_1^+ and p_2^-: as we show in appendix A the dependence on these momenta (and, hence, on the center-of-mass energy of the collision) comes in through singularities like $\delta(x^\pm = 0)$. For $t_2(x^+) \sim \delta'(x^+)$ one has

$$t_2 \frac{1}{\partial_+} t_2 \sim \delta'(x^+)\,\delta(x^+) \sim \left(\frac{\delta^2(x^+)}{2}\right)' \sim p_2^-\,\delta'(x^+). \tag{3.50}$$

Again we are not keeping track of factors not containing p_2^-. Iterating the procedure we get

$$\left(t_2 \frac{1}{\partial_+}\right)^n t_2 \sim (p_2^-)^n\,\delta'(x^+), \tag{3.51}$$

that is, for delta-prime shock waves $t_2\,(1/\partial_+) \sim p_2^-$.

To understand higher order terms with more powers of $1/\partial_+$ consider

$$t_2 \frac{1}{\partial_+^2} t_2 \sim \delta'(x^+)\theta(x^+) \sim \big(\delta(x^+)\theta(x^+)\big)' - \delta^2(x^+) \sim \big(\delta(x^+)\theta(x^+)\big)' - p_2^-\delta(x^+). \tag{3.52}$$

The term which was subleading for the delta-function shock waves (see eq. (3.49)) gives a leading-order factor of p_2^- for delta-prime shock waves, as we see from the last term in eq. (3.52). Applying higher powers of $t_2\,(1/\partial_+)$ to the last term in eq. (3.52) does not make the term less important:

$$\left(t_2\,\frac{1}{\partial_+}\right)^n\,p_2^-\,\delta(x^+)\;\sim\;(p_2^-)^{n+1}\,\delta(x^+). \tag{3.53}$$

(In fact the $(\delta(x^+)\,\theta(x^+))'$ term in eq. (3.52) also brings in powers of p_2^- after the operator $t_2\,(1/\partial_+)$ acts on it at least once.) We thus see that one insertion of $t_2(1/\partial_+^2)$ still gives leading terms in the case of delta-prime shock waves. Fortunately higher order insertions of $t_2(1/\partial_+^2)$ start generating subleading terms and can be discarded. We illustrate this by acting with $t_2(1/\partial_+^2)$ on the last term in eq. (3.52):

$$t_2\,\frac{1}{\partial_+^2}\,p_2^-\,\delta(x^+)\;\sim\;p_2^-\,\delta'(x^+)\,x^+\,\theta(x^+)\;\sim\;-p_2^-\,\delta(x^+)\,\theta(x^+). \tag{3.54}$$

No extra powers of p_2^- is generated and hence such terms are subleading.

Insertions of a higher number of inverse derivatives are also subleading. For instance

$$t_2\,\frac{1}{\partial_+^3}\,t_2\;\sim\;\delta'(x^+)\;x^+\,\theta(x^+)\;\sim\;-\delta(x^+)\,\theta(x^+), \tag{3.55}$$

again producing no powers of p_2^-.

We conclude that for delta-prime shock waves the eikonal approximation consists of the term in eq. (3.28) along with all terms with a single insertion of $t_2(1/\partial_+^2)$ in all possible positions.

3.4.2 Energy-momentum tensor of the produced medium

To take into account all leading terms for the delta-prime shock waves we write

$$\bar{h}\;=\;\bar{h}_{\rm eik}+\delta\bar{h} \tag{3.56}$$

with $\bar{h}_{\rm eik}$ given by eq. (3.28) and $\delta\bar{h}$ denoting the sum of all terms with all-orders of $t_2(1/\partial_+)$ and exactly one insertion of $t_2(1/\partial_+^2)$ as contained in eq. (3.23).

Expanding eq. (3.23) to the first order in $t_2(1/\partial_+^2)$ we write

$$\delta\bar{h}=\left[\left(1+\frac{1}{2}z^4t_2\frac{\partial_-}{\partial_+}\right)^2\right]^{-1}\left[\frac{1}{2}z^4t_2\frac{1}{\partial_+^2}\left(\hat{D}_1+\hat{D}_2\right)+\frac{1}{8}z^4t_2\frac{\partial_-}{\partial_+}z^4t_2\frac{1}{\partial_+^2}\hat{D}_1\right]\bar{h}_{\rm eik}. \tag{3.57}$$

Expanding the first factor on the right hand side of eq. (3.57) into a series and using the series representation for $\bar{h}_{\rm eik}$ from eq. (3.29) yields

$$\begin{aligned}\delta\bar{h}=&\sum_{m=0}^{\infty}(m+1)\left(-\frac{1}{2}z^4t_2\frac{\partial_-}{\partial_+}\right)^m\left[\frac{1}{2}z^4t_2\frac{1}{\partial_+^2}\left(\hat{D}_1+\hat{D}_2\right)+\frac{1}{8}z^4t_2\frac{\partial_-}{\partial_+}z^4t_2\frac{1}{\partial_+^2}\hat{D}_1\right]\\&\times\sum_{n=0}^{\infty}(n+1)\left(-\frac{1}{2}z^4t_2\frac{\partial_-}{\partial_+}\right)^n16z^7t_1t_2.\end{aligned} \tag{3.58}$$

Using the definitions of $\hat{D}_1$ and $\hat{D}_2$ from eqs. (3.19) and (3.20) we obtain

$$\hat{D}_1\, z^{4\,n+7} \;=\; -8\,(n+1)\,(2\,n+1)\, z^{4\,n+5} \tag{3.59}$$

and

$$\left(\hat{D}_1+\hat{D}_2\right)\, z^{4\,n+7} \;=\; -4\,(n+1)\,(2\,n+3)\, z^{4\,n+5}, \tag{3.60}$$

which allow us to rewrite eq. (3.58) as

$$\begin{aligned}\delta\bar{h} \;=& 16\,\sum_{n,m=0}^{\infty}(n+1)^2\,(m+1)\,\left(-\frac{1}{2}\right)^{n+m}\,\left(t_2\,\frac{1}{\partial_+}\right)^m\,\left[-2\,(2\,n+3)\,z^{4\,(n+m)+9}\,t_2\,\frac{1}{\partial_+^2}\right.\\ &\left.-(2\,n+1)\,z^{4\,(n+m)+13}\,\partial_-\,t_2\,\frac{1}{\partial_+}\,t_2\,\frac{1}{\partial_+^2}\right]\,\left[\partial_-^{n+m}t_1\right]\,\left(t_2\,\frac{1}{\partial_+}\right)^n\,t_2.\end{aligned} \tag{3.61}$$

The truncated amplitude contribution (3.61) leads to the contribution to the amplitude through eq. (3.25). Using the Green function (3.9) we write

$$\begin{aligned}\delta h =& 2z^2\int_{-\infty}^{x^+}dx'^+\int_{-\infty}^{x^-}dx'^-\int_0^{\infty}dz'\int_0^{\infty}dqqJ_0\left(q\sqrt{2(x^+-x'^+)(x^--x'^-)}\right)J_2(qz)J_2(qz')\\ &\times\sum_{n,m=0}^{\infty}(n+1)^2(m+1)\left(-\frac{1}{2}\right)^{n+m}\left(t_2(x'^+)\frac{1}{\partial'_+}\right)^m\\ &\times\left[-\frac{2(2n+3)}{n+m+2}(z')^{4(n+m)+7}t_2(x'^+)\frac{1}{\partial'^2_+}-\frac{2n+1}{n+m+3}(z')^{4(n+m)+11}\partial'_-t_2(x'^+)\frac{1}{\partial'_+}t_2(x'^+)\frac{1}{\partial'^2_+}\right]\\ &\times\left[\partial'^{n+m}_-t_1(x'^-)\right]\left(t_2(x'^+)\frac{1}{\partial'_+}\right)^n t_2(x'^+).\end{aligned} \tag{3.62}$$

As in section 3.3 we are interested in the contribution of the metric element, now the term δh, to the transverse pressure. As further evaluation of eq. (3.62) to all orders in z appears to be rather involved, we expand it to the order z^4 using eq. (3.31), integrate over z' and q, and eliminate the ∂'_- derivatives by successive integrations by parts. This yields the following contribution to the transverse pressure

$$\begin{aligned}\delta p \;=\; -\frac{N_c^2}{2\,\pi^2}\,8\int_{-\infty}^{x^+}dx'^+\int_{-\infty}^{x^-}dx'^-\sum_{n,m=0}^{\infty}(n+1)^2\,(m+1)\,(-2)^{n+m}\,(x^--x'^-)^{n+m+2}\,t_1(x'^-)\\ \times\,(x^+-x'^+)^{2\,(n+m)+2}\,\left[2\,(2\,n+3)\,\frac{(2\,(n+m)+3)!}{(n+m+2)!}\right.\\ \left.+\,4\,(2\,n+1)\,\frac{(2\,(n+m)+5)!}{(n+m+3)!}\,(x^+-x'^+)^2\,(x^--x'^-)\,t_2(x'^+)\,\frac{1}{\partial'_+}\right]\\ \times\,\left(t_2(x'^+)\,\frac{1}{\partial'_+}\right)^m\,t_2(x'^+)\,\frac{1}{\partial'^2_+}\,\left(t_2(x'^+)\,\frac{1}{\partial'_+}\right)^n\,t_2(x'^+).\end{aligned} \tag{3.63}$$

For further evaluation of eq. (3.63) we will explicitly substitute the shock wave profiles from eq. (2.33). As one can see from the calculations in appendix A the regularization in eq. (2.34) is not needed for the leading-p_2^- terms.

JHEP05(2009)060

First let us find the contribution to the transverse pressure coming from the piece in eq. (3.33), which we will refer to as $p_{\rm eik}$. As can be easily shown for t_2 from eq. (2.33) (see appendix B)

$$\left(t_2(x^+)\,\frac{1}{\partial_+}\right)^n t_2(x^+) \,=\, \frac{(\Lambda_2^2)^{n+1}}{(n+1)!}\,\left(\delta^{n+1}(x^+)\right)'. \tag{3.64}$$

In eq. (3.64) and henceforth for simplicity we absorb factors of $A_1^{1/3}$ and $A_2^{1/3}$ into Λ_1^2 and Λ_2^2. Using eqs. (2.33) and (3.64) in eq. (3.33) yields

$$p_{\rm eik} \,=\, \frac{N_c^2}{2\,\pi^2}\,8\,\Lambda_1^2\,\Lambda_2^2\,\theta(x^+)\,\theta(x^-)\,\frac{1-44\,p_2^-\,\Lambda_2^2\,(x^+)^2\,x^- + 64\,\left(p_2^-\,\Lambda_2^2\,(x^+)^2\,x^-\right)^2}{\left[1+8\,p_2^-\,\Lambda_2^2\,(x^+)^2\,x^-\right]^{7/2}}. \tag{3.65}$$

To evaluate eq. (3.63) one needs another relation (see appendix B for its derivation), valid only for t_2 from eq. (2.33) at the leading order in p_2^-

$$\left(t_2(x^+)\frac{1}{\partial_+}\right)^m t_2(x^+)\frac{1}{\partial_+^2}\left(t_2(x^+)\frac{1}{\partial_+}\right)^n t_2(x^+) = \frac{(-1)^{m+1}(\Lambda_2^2)^{n+m+2}(p_2^-)^{n+m+1}}{(n+1)!(m+1)!}\delta(x^+). \tag{3.66}$$

Using eqs. (2.33) and (3.64) in eq. (3.63) we get

$$\begin{aligned}\delta p =& \frac{N_c^2}{2\pi^2}8\Lambda_1^2\Lambda_2^2\theta(x^+)\theta(x^-)\\ &\times\left\{1-36p_2^-\Lambda_2^2(x^+)^2x^- - \frac{1-44p_2^-\Lambda_2^2(x^+)^2x^- + 64\left(p_2^-\Lambda_2^2(x^+)^2x^-\right)^2}{\left[1+8p_2^-\Lambda_2^2(x^+)^2x^-\right]^{7/2}}\right\}.\end{aligned} \tag{3.67}$$

The net transverse pressure is obtained by adding eqs. (3.65) and (3.67)

$$p \,=\, p_{\rm eik} + \delta p \,=\, \frac{N_c^2}{2\,\pi^2}\,8\,\Lambda_1^2\,\Lambda_2^2\,\theta(x^+)\,\theta(x^-)\,\left[1-36\,p_2^-\,\Lambda_2^2\,(x^+)^2\,x^-\right]. \tag{3.68}$$

This is the first main result of this section. Importantly all higher order terms cancel leaving us with the simple expression (3.68)! Note that eq. (3.68) is just a sum of the LO and NLO corrections (resumming leading powers of p_2^-), and thus it agrees with eq. (2.35). Namely it turns out that the NLO transverse pressure from eq. (2.35) taken at the leading-p_2^- accuracy gives us the full eikonal result for the proton-nucleus scattering problem with delta-prime shock waves.

Eq. (3.68) indeed has a limited region of applicability. As it was derived for the proton-nucleus approximation, similar to eq. (3.37) we must have

$$p_1^+\,\Lambda_1^2\,(x^-)^2\,x^+ \,\ll\, 1, \quad p_2^-\,\Lambda_2^2\,(x^+)^2\,x^- \,\sim\, 1, \tag{3.69}$$

to be able to neglect eikonal graviton exchanges with the proton shock wave. We also want to neglect the non-eikonal terms shown in eq. (2.35), which requires (see eq. (2.32))

$$\Lambda_1^2\,\tau^2 \,\ll\, 1, \quad \Lambda_2^2\,\tau^2 \,\ll\, 1. \tag{3.70}$$

JHEP05(2009)060

It appears that the region of applicability of eq. (3.68) is indeed somewhat limited and is confined to the region of large x^+ and small x^-, i.e., the region of space-time in the forward light cone bordering the proton shock wave. Still it is perhaps surprising to see that the pressure in eq. (3.68) can easily become negative at large enough x^+. As the pressure is negative we conclude that the system has not yet reached the ideal hydrodynamics state, similar to what happened to the delta-function shock waves in section 3.3.

The presence of negative pressure does not pose any problems by itself: negative pressure is known to arise in the early stages of heavy ion collisions when they are described in the Color Glass Condensate framework [24, 25]. Even in the strongly-coupled theory considered here, the LO part of the transverse pressure (2.35), when used in eq. (2.12), leads to negative pressure in the longitudinal direction [1]. In comparison, appearance of a negative energy density would be indeed worrisome and would indicate an unphysical situation. However, we can not calculate the energy density here, as the matter distribution is indeed rapidity-dependent and is not described by the ideal hydrodynamics: it is impossible to find the local rest frame of such medium to meaningfully talk about the energy density.

Therefore negative pressure in eq. (3.68) may be physical. One could interpret it as follows: when we chose the delta-prime shock waves of eq. (2.33) we "forced" the shock waves not to stop and to continue along the light cone trajectories. At the same time the produced strongly-interacting medium is still trying to pull them back together. As the shock waves are "artificially" pinned down to their light cones they do not stop, thus creating a negative pressure in the medium which tries to slow them down.

Using eqs. (3.68), (2.24) and (2.12) we construct all non-zero components of the energy-momentum tensor of the produced medium:

$$\langle T^{++} \rangle = \frac{N_c^2}{2\pi^2} \left[-8\,\Lambda_1^2\,\Lambda_2^2\,\delta(x^-)\,x^+\,\theta(x^+) + 96\,p_2^-\,\Lambda_1^2\,\Lambda_2^4\,(x^+)^3\,\theta(x^+)\,\theta(x^-) \right], \tag{3.71a}$$

$$\langle T^{--} \rangle = \frac{N_c^2}{2\pi^2} \left[-8\,\Lambda_1^2\,\Lambda_2^2\,\delta(x^+)\,x^-\,\theta(x^-) + 288\,p_2^-\,\Lambda_1^2\,\Lambda_2^4\,x^+\,\theta(x^+)\,(x^-)^2\,\theta(x^-) \right], \tag{3.71b}$$

$$\langle T^{+-} \rangle = \frac{N_c^2}{2\pi^2}\,8\,\Lambda_1^2\,\Lambda_2^2\,\theta(x^+)\,\theta(x^-)\,\left[1 - 36\,p_2^-\,\Lambda_2^2\,(x^+)^2\,x^-\right], \tag{3.71c}$$

$$\langle T^{ij} \rangle = \delta^{ij}\,\frac{N_c^2}{2\pi^2}\,8\,\Lambda_1^2\,\Lambda_2^2\,\theta(x^+)\,\theta(x^-)\,\left[1 - 36\,p_2^-\,\Lambda_2^2\,(x^+)^2\,x^-\right]. \tag{3.71d}$$

This is the second main result of this section.

3.5 Validity Range of the Perturbative Expansion

Before proceeding to the conclusions, let us check the validity range of the perturbative approach for solving Einstein equations followed throughout the paper and outlined in eq. (2.14). For the sake of simplicity, we will explicitly analyze the relative contribution to the $\perp\perp$ metric coefficient obtained at LO ($H^{(0)}$), and NLO ($H^{(1)}$), for the case of (physical) delta function shock waves of eq. (2.26). Starting from eq. (2.15) for the LO results and eqs. (2.22)–(2.23) for the NLO one and dropping some trivial factors of order one, the ratio $R_{NLO/LO}$ between the NLO and LO contribution to the metric coefficient $H(x^+, x^-, z)$ is

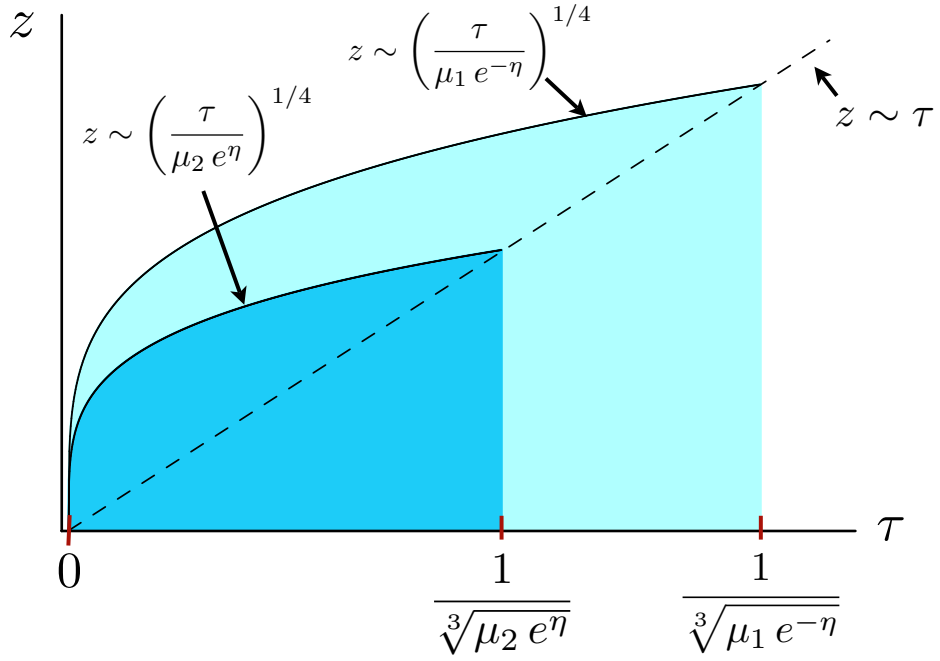

Figure 8. Schematic plot of the validity range of our solution in the z-τ plane. The z-axis was moved to a slight left of $\tau = 0$ line for illustrative purposes only: indeed $\tau \geq 0$. The darker shaded area indicated the validity region of the perturbative expansion of section 2. The lighter shaded area (together with the darker one) depicts the broader validity region of the pA approximation developed in this section.

given by

$$R_{NLO/LO} \equiv \frac{H^{(1)}(x^+, x^-, z)}{H^{(0)}(x^+, x^-, z)} \sim \mu_2\, \tau^3\, e^{\eta}\, \frac{1 + (z/\tau)^2 + (z/\tau)^4 + (z/\tau)^6}{1 + (z/\tau)^2}. \tag{3.72}$$

For definitiveness we have chosen to concentrate on the higher order corrections due to graviton exchanges with the shock wave described by the energy scale μ_2. To obtain an estimate for the NLO graviton exchanges in the other shock wave one simply has to replace $\mu_2 \to \mu_1$ and $\eta \to -\eta$ in eq. (3.72). In arriving at eq. (3.72) we have made use of the relation $x^+ = \tau\, e^{\eta}/\sqrt{2}$, with $\eta = (1/2)\ln(x^+/x^-)$ the space-time rapidity. Note that all the coefficients in the numerator and denominator in the ratio in eq. (3.72) are put to be equal to 1 for simplicity of the parametric estimate we are performing.

Similar to eq. (3.72), one can build the ratio of the NNLO contribution, $H^{(2)}$ given by eqs. (2.38)–(2.39), to the NLO one $H^{(1)}$, again for the delta-function shock waves:

$$R_{NNLO/NLO} \equiv \frac{H^{(2)}(x^+, x^-, z)}{H^{(1)}(x^+, x^-, z)} \sim \mu_2 \tau^3 e^{\eta} \frac{1 + (z/\tau)^2 + (z/\tau)^4 + (z/\tau)^6}{1 + (z/\tau)^2} \sim R_{NLO/LO}. \tag{3.73}$$

One can easily show that eqs. (3.72) and (3.73) are also valid for delta-prime shock waves of eq. (2.33). Thus, the condition $R_{NLO/LO} \lesssim 1$ sets the validity range of the whole perturbative expansion. Two different situations can be considered: (*i*) $z \ll \tau$: in this case

JHEP05(2009)060

the perturbative expansion is justified as long as $\tau \lesssim [1/(\mu_2\, e^{\eta})]^{1/3}$. (ii) $z \gg \tau$: in this case $R_{NLO/LO} \lesssim 1$ if $z \lesssim [\tau/(\mu_2\, e^{\eta})]^{1/4}$. The validity region of our perturbative expansion given by the union of regions (i) and (ii) is depicted in figure 8 (see the darker shaded region there). Thus our approximation is valid in comparable intervals in τ and z near the boundary of the AdS space.

On the other hand, in the calculation performed in this section for asymmetric pA collisions, we resummed *all-order* graviton exchanges with the nucleus shock wave. Therefore the applicability of this approximation does not require $R_{NLO/LO} \lesssim 1$ for higher order corrections bringing in powers of μ_2. We do neglect all higher-order graviton exchanges with the proton shock wave that bring in higher powers of μ_1. Thus our pA approximation is valid only if $R_{NLO/LO} \lesssim 1$ for NLO corrections with $\mu_2 \to \mu_1$ and $\eta \to -\eta$ in eq. (3.72). The two regions (i) and (ii) become:

(i) $z \ll \tau$, $\tau \lesssim [1/(\mu_1\, e^{-\eta})]^{1/3}$, and

(ii) $z \gg \tau$, $z \lesssim [\tau/(\mu_1\, e^{-\eta})]^{1/4}$.

These new regions (i) and (ii) for pA collisions are shown in figure 8 by the lightly shaded area. Indeed the validity of the pA approximation is much broader than that of the validity of the perturbation series of section 2.

Importantly, the stopping time estimated in section 3.3.2, $\tau_{\rm stop} \sim [1/(\mu_2 e^{\eta})]^{1/3}$, lies within the validity range of our approximation, as one can easily see from figure 8. Our approach is valid for a comparably broad range of z's at the stopping time, though for the physics of the gauge theory in four dimensions only the knowledge of the metric in the small-z region is needed.

4 Conclusions

Let us summarize our main results. In section 2 we constructed the NLO and NNLO terms in the perturbative expansion in graviton exchanges for the collision of two shock waves. Our expansion generalizes similar expansion constructed previously in [12] from the delta-function-only case considered in [12] to the case of shock waves of arbitrary profile. In particular we see that even the delta-prime shock waves, which at LO gave rapidity-independent distribution of matter [1], lead to rapidity-dependent energy-momentum tensor at NLO (see eq. (2.35)).

It is worthwhile noting that the perturbative graviton expansion of section 2 can be built consistently without introducing a dilaton field. Hence at all orders of the solution the dilaton field is zero. As the dilaton field is dual to the $\langle {\rm tr} F^2_{\mu\nu}\rangle$ operator in the gauge theory at the boundary we conclude that for the collisions of shock waves considered here

$$\langle {\rm tr} F^2_{\mu\nu}\rangle \,=\, 0 \tag{4.1}$$

at all times. Thus electric and magnetic modes are always equilibrated in this strongly-coupled medium. This result should be contrasted with that of [53], where dilaton field was needed to construct singularity-free pre-asymptotics to the Bjorken hydrodynamics

JHEP05(2009)060

metric of [51]. As our calculations show, the absence of a dilaton field in the initial shock waves leads to no dilaton field throughout the collision. As it is difficult to construct shock waves with non-zero dilaton field it is not clear how to construct shock wave collisions with non-zero dilaton field in the forward light cone. Therefore the no-dilaton aspect of our result may give one reasons to worry whether dual-Bjorken geometry of [51] is obtainable at all in collisions of AdS shock waves.

In section 3 we have devised an eikonal resummation procedure, which resumed all graviton rescattering in one nucleus while keeping only one graviton exchange with another nucleus. The results for delta-function shock waves are given in eq. (3.38). As is clear from eq. (3.38) the matter distribution obtained in the proton-nucleus approximation can not be described by ideal hydrodynamics, and should be viewed as some intermediate stage of the matter evolution towards isotropization. We also showed explicitly in section 3 that strong interactions with the nucleus stop the proton completely, as can be seen from eq. (3.45).

The eikonal expansion for an asymmetric collision of two delta-prime shock waves terminates at the level of two graviton-exchange with the nucleus. The results of the resummation are shown in eq. (3.71). It is important to note that the energy-momentum tensors for delta-function shock waves (3.38) and for delta-primes (3.71) are strongly rapidity-dependent. It is unlikely that a matter distribution which is strongly rapidity-dependent at early times would become rapidity-independent at late times: such behavior would be acausal, as different rapidity regions become causally disconnected from each other as the collision evolves. It is therefore probable that collisions of shock waves in AdS will lead to a rapidity-dependent final state at late times: if, due to strong interactions, the matter in this late-time state would be described by the ideal hydrodynamics, this hydrodynamic description can not be that of rapidity-independent Bjorken hydrodynamics [30]. While a full (possibly numerical) study of the nucleus-nucleus collision in AdS would provide definitive answer to this question, it is possible that Bjorken geometry gives a good approximation to the dynamics of the matter produced in a collision of two identical nuclei only in a narrow interval around mid-rapidity. Our results here can serve as a benchmark for further (possibly numerical) studies of the collision of two shock waves beyond the asymmetric approximation done here.

It may be that to obtain Bjorken hydrodynamics in a broader rapidity range one has to abandon the idea of colliding shock waves in AdS, and try to simulate the initial stage of the medium by matching the AdS metric onto the results for the energy-momentum tensor known from weak-coupling CGC methods [24–29]. Such approach was advocated in [14, 28, 75] and may prove to be quite fruitful. One possible shortcoming of the matching method is in the fact that it leaves too much freedom in the choice of the early-time AdS metric, leading to a possible loss of uniqueness in the description of the subsequent time-evolution of the system. Further research is needed to understand which AdS approach is better suited to describe heavy ion collisions.

Acknowledgments

We would like to thank Samir Mathur and Robert Myers for informative discussions.

JHEP05(2009)060

The work of Yu.K. and A.T. is sponsored in part by the U.S. Department of Energy under Grant No. DE-FG02-05ER41377.

A Transverse pressure for delta-primes at NLO

We want to find the NLO contribution to the transverse pressure due to delta-prime sources. Using eq. (2.25) we write

$$p_{\rm NLO} \,=\, \frac{N_c^2}{2\,\pi^2}\,H_0^{(1)}(x^+,x^-) \,=\, \frac{N_c^2}{2\,\pi^2}\left[-\frac{6}{(\partial_+\,\partial_-)^2}\,\psi_7 - \frac{96}{(\partial_+\,\partial_-)^3}\,\psi_9 - \frac{2880}{(\partial_+\,\partial_-)^4}\,\psi_{11}\right] \quad \text{(A.1)}$$

where we used $H_0^{(1)}$ given by eq. (2.23a). Our goal is to evaluate the right hand side of eq. (A.1) for t_1 and t_2 given by eq. (2.34). For simplicity we will evaluate the terms with one power of t_1 only: the remaining terms with only one power of t_2 can be obtained by the substitution $t_1 \leftrightarrow t_2$.

Using eqs. (2.19) along with eqs. (2.16) we write

$$-\frac{6}{(\partial_+\,\partial_-)^2}\,\psi_7 \,=\, -64\,\left[\frac{1}{\partial_-^3}t_1(x^-)\right]\,\left[\frac{1}{\partial_+^2}t_2(x^+)\,\frac{1}{\partial_+^3}t_2(x^+)\right] + (t_1 \leftrightarrow t_2). \quad \text{(A.2)}$$

Using eq. (2.34) we get

$$\frac{1}{\partial_-^3}t_1(x^-) \,=\, \Lambda_1^2\sum_{i=1}^{A_1^{1/3}}(x^- - x_i^-)\,\theta(x^- - x_i^-) \,\approx\, \Lambda_1^2\,A_1^{1/3}\,x^-\,\theta(x^-) \quad \text{(A.3)}$$

for $x^- \gg a_1$. Similarly we write

$$\begin{aligned}\frac{1}{\partial_+^2}t_2(x^+)\frac{1}{\partial_+^3}t_2(x^+) &= \Lambda_2^4\sum_{i,j=1}^{A_2^{1/3}}\int_{-\infty}^{x^+}dx'^+\int_{-\infty}^{x'^+}dx''^+\delta'(x''^+ - x_i^+)(x''^+ - x_j^+)\theta(x''^+ - x_j^+)\\ &= \Lambda_2^4\sum_{i,j=1}^{A_2^{1/3}}\int_{-\infty}^{x^+}dx'^+\left[\delta(x'^+ - x_i^+)(x_i^+ - x_j^+)\theta(x_i^+ - x_j^+) - \theta(x'^+ - x_i^+)\theta(x_i^+ - x_j^+)\right]\\ &\approx \frac{(\Lambda_2^2 A_2^{1/3})^2}{2}x^+\theta(x^+), \end{aligned} \quad \text{(A.4)}$$

where in the last step we have used $x^+ \gg a_2$. Combining eqs. (A.3) and (A.4) we obtain

$$-\frac{6}{(\partial_+\,\partial_-)^2}\,\psi_7 \,\approx\, -32\,\Lambda_1^2\,A_1^{1/3}\,(\Lambda_2^2\,A_2^{1/3})^2\,x^+\,x^-\,\theta(x^+)\,\theta(x^-) + (1 \leftrightarrow 2). \quad \text{(A.5)}$$

Eqs. (2.19), (2.16) give

$$-\frac{96}{(\partial_+\,\partial_-)^3}\,\psi_9 \,=\, -576\,\left[\frac{1}{\partial_-^3}t_1(x^-)\right]\,\left[\frac{1}{\partial_+^3}t_2(x^+)\,\frac{1}{\partial_+^2}t_2(x^+)\right] + (t_1 \leftrightarrow t_2). \quad \text{(A.6)}$$

The only difference of eq. (A.6) with eq. (A.2) is in t_2-dependent part, which is evaluated to give

$$\frac{1}{\partial_+^3}t_2(x^+)\frac{1}{\partial_+^2}t_2(x^+) = \Lambda_2^4\sum_{i,j=1}^{A_2^{1/3}}\int_{-\infty}^{x^+}dx'^+\int_{-\infty}^{x'^+}dx''^+\int_{-\infty}^{x''^+}dx'''^+\delta'(x'''^+ - x_i^+)\theta(x'''^+ - x_j^+)$$
$$= \Lambda_2^4\sum_{i,j=1}^{A_2^{1/3}}\int_{-\infty}^{x^+}dx'^+\int_{-\infty}^{x'^+}dx''^+\int_{-\infty}^{x''^+}dx'''^+$$
$$\times\left[\partial_+'''\left(\delta(x'''^+ - x_i^+)\theta(x'''^+ - x_j^+)\right) - \delta(x'''^+ - x_i^+)\delta(x'''^+ - x_j^+)\right]. \tag{A.7}$$

The last term in the last line of eq. (A.7) is only non-zero when $x_i^+ = x_j^+$, which is only true if $i = j$ as all the x_i^+'s are different. However, if $i = j$ that term becomes a delta-function squared. Regulating the infinity by the largest momentum scale in the problem we replace $\delta(x^+ = 0) \to p_2^-$ and get

$$\frac{1}{\partial_+^3}t_2(x^+)\frac{1}{\partial_+^2}t_2(x^+) = \Lambda_2^4\sum_{i,j=1}^{A_2^{1/3}}\int_{-\infty}^{x^+}dx'^+\int_{-\infty}^{x'^+}dx''^+$$
$$\times\left[\delta(x''^+ - x_i^+)\theta(x_i^+ - x_j^+) - \delta_{ij}p_2^-\theta(x''^+ - x_i^+)\right]$$
$$\approx \frac{(\Lambda_2^2 A_2^{1/3})^2}{2}x^+\theta(x^+)\left[1 - \frac{p_2^- x^+}{A_2^{1/3}}\right] \tag{A.8}$$

for $x^+ \gg a_2$. Combining eqs. (A.3) and (A.8) in eq. (A.6) we get

$$-\frac{96}{(\partial_+\partial_-)^3}\psi_9 = -288\Lambda_1^2 A_1^{1/3}(\Lambda_2^2 A_2^{1/3})^2 x^+x^-\theta(x^+)\theta(x^-)$$
$$\times\left[1 - \frac{p_2^- x^+}{A_2^{1/3}}\right] + (1 \leftrightarrow 2, + \leftrightarrow -). \tag{A.9}$$

(Indeed the delta function $\delta(x^- = 0)$ should be regulated by p_1^+.)

Similar to the above one gets

$$-\frac{2880}{(\partial_+\,\partial_-)^4}\,\psi_{11} \;=\; -2304\,\left[\frac{1}{\partial_-^3}t_1(x^-)\right]\,\left[\frac{1}{\partial_+^4}t_2(x^+)\,\frac{1}{\partial_+}t_2(x^+)\right] + (t_1 \leftrightarrow t_2)$$
$$=\; -576\,\Lambda_1^2\,A_1^{1/3}\,(\Lambda_2^2\,A_2^{1/3})^2\,x^+\,x^-\,\theta(x^+)\,\theta(x^-)\,\frac{p_2^-\,x^+}{A_2^{1/3}} + (1 \leftrightarrow 2,\, + \leftrightarrow -). \tag{A.10}$$

Using eqs. (A.5), (A.9), and (A.10) in eq. (A.1) yields the NLO contribution to the pressure given in eq. (2.35).

B Iterations of delta-primes

We start by proving eq. (3.64) for

$$t_2(x^+) \;=\; \Lambda_2^2\,\delta'(x^+). \tag{B.1}$$

Evaluating one iteration of $t_2(1/\partial_+)$ operator acting on t_2 we get

$$t_2(x^+)\,\frac{1}{\partial_+}\,t_2(x^+) \;=\; (\Lambda_2^2)^2\,\delta'(x^+)\,\delta(x^+) \;=\; (\Lambda_2^2)^2\,\left(\frac{\delta^2(x^+)}{2}\right)'. \tag{B.2}$$

Similarly

$$\left(t_2(x^+)\,\frac{1}{\partial_+}\right)^2 t_2(x^+) \;=\; (\Lambda_2^2)^3\,\delta'(x^+)\,\frac{\delta^2(x^+)}{2} \;=\; (\Lambda_2^2)^3\,\left(\frac{\delta^3(x^+)}{3!}\right)'. \tag{B.3}$$

It is now straightforward to see what happens at each step of application of the $t_2(1/\partial_+)$ operator to write

$$\left(t_2(x^+)\,\frac{1}{\partial_+}\right)^n t_2(x^+) \;=\; \frac{(\Lambda_2^2)^{n+1}}{(n+1)!}\,\left(\delta^{n+1}(x^+)\right)', \tag{B.4}$$

which is exactly eq. (3.64), as desired.

Now let us prove eq. (3.66) for t_2 from eq. (B.1). First of all use eq. (B.4) that we just proved to write

$$\left(t_2(x^+)\frac{1}{\partial_+}\right)^m t_2(x^+)\frac{1}{\partial_+^2}\left(t_2(x^+)\frac{1}{\partial_+}\right)^n t_2(x^+) = \frac{(\Lambda_2^2)^{n+1}}{(n+1)!}\left(t_2(x^+)\frac{1}{\partial_+}\right)^{m+1}\delta^{n+1}(x^+). \tag{B.5}$$

To evaluate

$$\left(t_2(x^+)\,\frac{1}{\partial_+}\right)^{m+1}\delta^{n+1}(x^+) \tag{B.6}$$

we write

$$\begin{aligned}\left(\delta'(x^+)\frac{1}{\partial_+}\right)^{m+1} &= \delta'(x^+)\frac{1}{\partial_+}\delta'(x^+)\frac{1}{\partial_+}\ldots\delta'(x^+)\frac{1}{\partial_+} = -\left(\frac{\delta^2(x^+)}{2}\right)'\frac{1}{\partial_+}\left(\delta'(x^+)\frac{1}{\partial_+}\right)^{m-1}\\ &= \left(\frac{\delta^3(x^+)}{3!}\right)'\frac{1}{\partial_+}\left(\delta'(x^+)\frac{1}{\partial_+}\right)^{m-2} = \ldots = (-1)^m\left(\frac{\delta^{m+1}(x^+)}{(m+1)!}\right)'\frac{1}{\partial_+}.\end{aligned} \tag{B.7}$$

In each step in eq. (B.7) we neglected a total derivative: it can be shown that those total derivatives do not generate leading powers of p_2^-. Eq. (B.7) gives

$$\begin{aligned}&\left(t_2(x^+)\frac{1}{\partial_+}\right)^{m+1}\delta^{n+1}(x^+) = (\Lambda_2^2)^{m+1}(-1)^m\left(\frac{\delta^{m+1}(x^+)}{(m+1)!}\right)'\frac{1}{\partial_+}\delta^{n+1}(x^+)\\ &= \frac{(-1)^{m+1}(\Lambda_2^2)^{m+1}}{(m+1)!}\delta^{n+m+2}(x^+) = \frac{(-1)^{m+1}(\Lambda_2^2)^{m+1}(p_2^-)^{n+m+1}}{(m+1)!}\delta(x^+),\end{aligned} \tag{B.8}$$

where we again neglected the total derivative as it is subleading. In eq. (B.8) we have also regularized the extra powers of $\delta(x^+=0)$ by replacing them with p_2^-.

Combining eqs. (B.8) and (B.5) yields

$$\left(t_2(x^+)\frac{1}{\partial_+}\right)^m t_2(x^+)\frac{1}{\partial_+^2}\left(t_2(x^+)\frac{1}{\partial_+}\right)^n t_2(x^+) = \frac{(-1)^{m+1}(\Lambda_2^2)^{n+m+2}(p_2^-)^{n+m+1}}{(n+1)!\;(m+1)!}\delta(x^+), \tag{B.9}$$

which is exactly eq. (3.66).

JHEP05(2009)060

References

[1] J.L. Albacete, Y.V. Kovchegov and A. Taliotis, *Modeling heavy ion collisions in AdS/CFT*, *JHEP* **07** (2008) 100 [arXiv:0805.2927] [SPIRES].

[2] J.M. Maldacena, *The large-N limit of superconformal field theories and supergravity*, *Adv. Theor. Math. Phys.* **2** (1998) 231 [*Int. J. Theor. Phys.* **38** (1999) 1113] [hep-th/9711200] [SPIRES].

[3] S.S. Gubser, I.R. Klebanov and A.M. Polyakov, *Gauge theory correlators from non-critical string theory*, *Phys. Lett.* **B 428** (1998) 105 [hep-th/9802109] [SPIRES].

[4] E. Witten, *Anti-de Sitter space and holography*, *Adv. Theor. Math. Phys.* **2** (1998) 253 [hep-th/9802150] [SPIRES].

[5] O. Aharony, S.S. Gubser, J.M. Maldacena, H. Ooguri and Y. Oz, *Large-N field theories, string theory and gravity*, *Phys. Rept.* **323** (2000) 183 [hep-th/9905111] [SPIRES].

[6] P.D. D'Eath and P.N. Payne, *Gravitational radiation in high speed black hole collisions. 1. Perturbation treatment of the axisymmetric speed of light collision*, *Phys. Rev.* **D 46** (1992) 658 [SPIRES].

[7] P.D. D'Eath and P.N. Payne, *Gravitational radiation in high speed black hole collisions. 2. Reduction to two independent variables and calculation of the second order news function*, *Phys. Rev.* **D 46** (1992) 675 [SPIRES].

[8] P.D. D'Eath and P.N. Payne, *Gravitational radiation in high speed black hole collisions. 3. Results and conclusions*, *Phys. Rev.* **D 46** (1992) 694 [SPIRES].

[9] U. Sperhake, V. Cardoso, F. Pretorius, E. Berti and J.A. Gonzalez, *The high-energy collision of two black holes*, *Phys. Rev. Lett.* **101** (2008) 161101 [arXiv:0806.1738] [SPIRES].

[10] H. Nastase, *The RHIC fireball as a dual black hole*, hep-th/0501068 [SPIRES].

[11] K. Kajantie, J. Louko and T. Tahkokallio, *Gravity dual of conformal matter collisions in $1+1$ dimensions*, *Phys. Rev.* **D 77** (2008) 066001 [arXiv:0801.0198] [SPIRES].

[12] D. Grumiller and P. Romatschke, *On the collision of two shock waves in AdS_5*, *JHEP* **08** (2008) 027 [arXiv:0803.3226] [SPIRES].

[13] S.S. Gubser, S.S. Pufu and A. Yarom, *Entropy production in collisions of gravitational shock waves and of heavy ions*, *Phys. Rev.* **D 78** (2008) 066014 [arXiv:0805.1551] [SPIRES].

[14] S. Lin and E. Shuryak, *Grazing collisions of gravitational shock waves and entropy production in heavy ion collision*, arXiv:0902.1508 [SPIRES].

[15] P.F. Kolb, J. Sollfrank and U.W. Heinz, *Anisotropic transverse flow and the quark-hadron phase transition*, *Phys. Rev.* **C 62** (2000) 054909 [hep-ph/0006129] [SPIRES].

[16] P.F. Kolb, P. Huovinen, U.W. Heinz and H. Heiselberg, *Elliptic flow at SPS and RHIC: from kinetic transport to hydrodynamics*, *Phys. Lett.* **B 500** (2001) 232 [hep-ph/0012137] [SPIRES].

[17] P. Huovinen, P.F. Kolb, U.W. Heinz, P.V. Ruuskanen and S.A. Voloshin, *Radial and elliptic flow at RHIC: further predictions*, *Phys. Lett.* **B 503** (2001) 58 [hep-ph/0101136] [SPIRES].

[18] P.F. Kolb, U.W. Heinz, P. Huovinen, K.J. Eskola and K. Tuominen, *Centrality dependence of multiplicity, transverse energy, and elliptic flow from hydrodynamics*, *Nucl. Phys.* **A 696** (2001) 197 [hep-ph/0103234] [SPIRES].

JHEP05(2009)060

[19] U.W. Heinz and P.F. Kolb, *Early thermalization at RHIC*, *Nucl. Phys.* **A 702** (2002) 269 [hep-ph/0111075] [SPIRES].

[20] D. Teaney and E.V. Shuryak, *An unusual space-time evolution for heavy ion collisions at high energies due to the QCD phase transition*, *Phys. Rev. Lett.* **83** (1999) 4951 [nucl-th/9904006] [SPIRES].

[21] D. Teaney, J. Lauret and E.V. Shuryak, *Flow at the SPS and RHIC as a quark gluon plasma signature*, *Phys. Rev. Lett.* **86** (2001) 4783 [nucl-th/0011058] [SPIRES].

[22] D. Teaney, J. Lauret and E.V. Shuryak, *A hydrodynamic description of heavy ion collisions at the SPS and RHIC*, nucl-th/0110037 [SPIRES].

[23] D. Teaney, *Effect of shear viscosity on spectra, elliptic flow and Hanbury Brown-Twiss radii*, *Phys. Rev.* **C 68** (2003) 034913 [nucl-th/0301099] [SPIRES].

[24] A. Krasnitz, Y. Nara and R. Venugopalan, *Classical gluodynamics of high energy nuclear collisions: an erratum and an update*, *Nucl. Phys.* **A 727** (2003) 427 [hep-ph/0305112] [SPIRES].

[25] A. Krasnitz, Y. Nara and R. Venugopalan, *Gluon production in the color glass condensate model of collisions of ultrarelativistic finite nuclei*, *Nucl. Phys.* **A 717** (2003) 268 [hep-ph/0209269] [SPIRES].

[26] T. Lappi, *Production of gluons in the classical field model for heavy ion collisions*, *Phys. Rev.* **C 67** (2003) 054903 [hep-ph/0303076] [SPIRES].

[27] K. Fukushima, *Initial fields and instability in the classical model of the heavy-ion collision*, *Phys. Rev.* **C 76** (2007) 021902 [*Erratum ibid.* **C 77** (2007) 029901] [arXiv:0704.3625] [SPIRES].

[28] Y.V. Kovchegov and A. Taliotis, *Early time dynamics in heavy ion collisions from AdS/CFT correspondence*, *Phys. Rev.* **C 76** (2007) 014905 [arXiv:0705.1234] [SPIRES].

[29] Y.V. Kovchegov, *Can thermalization in heavy ion collisions be described by QCD diagrams?*, *Nucl. Phys.* **A 762** (2005) 298 [hep-ph/0503038] [SPIRES].

[30] J.D. Bjorken, *Highly relativistic nucleus-nucleus collisions: the central rapidity region*, *Phys. Rev.* **D 27** (1983) 140 [SPIRES].

[31] J.P. Blaizot and A.H. Mueller, *The early stage of ultrarelativistic heavy ion collisions*, *Nucl. Phys.* **B 289** (1987) 847 [SPIRES].

[32] L.D. McLerran and R. Venugopalan, *Computing quark and gluon distribution functions for very large nuclei*, *Phys. Rev.* **D 49** (1994) 2233 [hep-ph/9309289] [SPIRES].

[33] L.D. McLerran and R. Venugopalan, *Gluon distribution functions for very large nuclei at small transverse momentum*, *Phys. Rev.* **D 49** (1994) 3352 [hep-ph/9311205] [SPIRES].

[34] L.D. McLerran and R. Venugopalan, *Green's functions in the color field of a large nucleus*, *Phys. Rev.* **D 50** (1994) 2225 [hep-ph/9402335] [SPIRES].

[35] Y.V. Kovchegov, *Non-Abelian Weizsaecker-Williams field and a two-dimensional effective color charge density for a very large nucleus*, *Phys. Rev.* **D 54** (1996) 5463 [hep-ph/9605446] [SPIRES].

[36] Y.V. Kovchegov, *Quantum structure of the non-Abelian Weizsaecker-Williams field for a very large nucleus*, *Phys. Rev.* **D 55** (1997) 5445 [hep-ph/9701229] [SPIRES].

JHEP05(2009)060

[37] A. Kovner, L.D. McLerran and H. Weigert, *Gluon production from nonAbelian Weizsacker-Williams fields in nucleus-nucleus collisions*, *Phys. Rev.* **D 52** (1995) 6231 [hep-ph/9502289] [SPIRES].

[38] Y.V. Kovchegov and D.H. Rischke, *Classical gluon radiation in ultrarelativistic nucleus nucleus collisions*, *Phys. Rev.* **C 56** (1997) 1084 [hep-ph/9704201] [SPIRES].

[39] A. Krasnitz and R. Venugopalan, *Non-perturbative computation of gluon mini-jet production in nuclear collisions at very high energies*, *Nucl. Phys.* **B 557** (1999) 237 [hep-ph/9809433] [SPIRES].

[40] A. Krasnitz and R. Venugopalan, *The initial energy density of gluons produced in very high energy nuclear collisions*, *Phys. Rev. Lett.* **84** (2000) 4309 [hep-ph/9909203] [SPIRES].

[41] Y.V. Kovchegov, *Classical initial conditions for ultrarelativistic heavy ion collisions*, *Nucl. Phys.* **A 692** (2001) 557 [hep-ph/0011252] [SPIRES].

[42] D. Kharzeev and M. Nardi, *Hadron production in nuclear collisions at RHIC and high density QCD*, *Phys. Lett.* **B 507** (2001) 121 [nucl-th/0012025] [SPIRES].

[43] D. Kharzeev, E. Levin and M. Nardi, *The onset of classical QCD dynamics in relativistic heavy ion collisions*, *Phys. Rev.* **C 71** (2005) 054903 [hep-ph/0111315] [SPIRES].

[44] D. Kharzeev, E. Levin and L. McLerran, *Parton saturation and N(part) scaling of semi-hard processes in QCD*, *Phys. Lett.* **B 561** (2003) 93 [hep-ph/0210332] [SPIRES].

[45] D. Kharzeev, Y.V. Kovchegov and K. Tuchin, *Nuclear modification factor in $d + Au$ collisions: onset of suppression in the color glass condensate*, *Phys. Lett.* **B 599** (2004) 23 [hep-ph/0405045] [SPIRES].

[46] J.L. Albacete, N. Armesto, A. Kovner, C.A. Salgado and U.A. Wiedemann, *Energy dependence of the Cronin effect from non-linear QCD evolution*, *Phys. Rev. Lett.* **92** (2004) 082001 [hep-ph/0307179] [SPIRES].

[47] J.L. Albacete, *Particle multiplicities in lead-lead collisions at the LHC from non-linear evolution with running coupling*, *Phys. Rev. Lett.* **99** (2007) 262301 [arXiv:0707.2545] [SPIRES].

[48] E. Iancu and R. Venugopalan, *The color glass condensate and high energy scattering in QCD*, hep-ph/0303204 [SPIRES].

[49] H. Weigert, *Evolution at small x_{bj}: the color glass condensate*, *Prog. Part. Nucl. Phys.* **55** (2005) 461 [hep-ph/0501087] [SPIRES].

[50] J. Jalilian-Marian and Y.V. Kovchegov, *Saturation physics and deuteron gold collisions at RHIC*, *Prog. Part. Nucl. Phys.* **56** (2006) 104 [hep-ph/0505052] [SPIRES].

[51] R.A. Janik and R.B. Peschanski, *Asymptotic perfect fluid dynamics as a consequence of AdS/CFT*, *Phys. Rev.* **D 73** (2006) 045013 [hep-th/0512162] [SPIRES].

[52] R.A. Janik, *Viscous plasma evolution from gravity using AdS/CFT*, *Phys. Rev. Lett.* **98** (2007) 022302 [hep-th/0610144] [SPIRES].

[53] M.P. Heller and R.A. Janik, *Viscous hydrodynamics relaxation time from AdS/CFT*, *Phys. Rev.* **D 76** (2007) 025027 [hep-th/0703243] [SPIRES].

[54] P. Benincasa, A. Buchel, M.P. Heller and R.A. Janik, *On the supergravity description of boost invariant conformal plasma at strong coupling*, *Phys. Rev.* **D 77** (2008) 046006 [arXiv:0712.2025] [SPIRES].

JHEP05(2009)060

[55] M.P. Heller, P. Surowka, R. Loganayagam, M. Spalinski and S.E. Vazquez, *On a consistent AdS/CFT description of boost-invariant plasma*, arXiv:0805.3774 [SPIRES].

[56] A. Kovner, L.D. McLerran and H. Weigert, *Gluon production at high transverse momentum in the McLerran-Venugopalan model of nuclear structure functions*, *Phys. Rev.* **D 52** (1995) 3809 [hep-ph/9505320] [SPIRES].

[57] L.D. Landau, *On the multiparticle production in high-energy collisions* (in Russian), *Izv. Akad. Nauk SSSR Ser. Fiz.* **17** (1953) 51 [SPIRES].

[58] BRAHMS collaboration, I.G. Bearden et al., *Nuclear stopping in Au + Au collisions at* $\sqrt{s_{\rm NN}} = 200$ *GeV*, *Phys. Rev. Lett.* **93** (2004) 102301 [nucl-ex/0312023] [SPIRES].

[59] K. Itakura, Y.V. Kovchegov, L. McLerran and D. Teaney, *Baryon stopping and valence quark distribution at small x*, *Nucl. Phys.* **A 730** (2004) 160 [hep-ph/0305332] [SPIRES].

[60] J.L. Albacete and Y.V. Kovchegov, *Baryon stopping in proton nucleus collisions*, *Nucl. Phys.* **A 781** (2007) 122 [hep-ph/0605053] [SPIRES].

[61] Y.V. Kovchegov and A.H. Mueller, *Gluon production in current nucleus and nucleon nucleus collisions in a quasi-classical approximation*, *Nucl. Phys.* **B 529** (1998) 451 [hep-ph/9802440] [SPIRES].

[62] B.Z. Kopeliovich, A.V. Tarasov and A. Schafer, *Bremsstrahlung of a quark propagating through a nucleus*, *Phys. Rev.* **C 59** (1999) 1609 [hep-ph/9808378] [SPIRES].

[63] A. Dumitru and L.D. McLerran, *How protons shatter colored glass*, *Nucl. Phys.* **A 700** (2002) 492 [hep-ph/0105268] [SPIRES].

[64] Y.V. Kovchegov and K. Tuchin, *Inclusive gluon production in DIS at high parton density*, *Phys. Rev.* **D 65** (2002) 074026 [hep-ph/0111362] [SPIRES].

[65] Y.V. Kovchegov, *Diffractive gluon production in proton nucleus collisions and in DIS*, *Phys. Rev.* **D 64** (2001) 114016 [*Erratum ibid.* **D 68** (2003) 039901] [hep-ph/0107256] [SPIRES].

[66] R.C. Brower, M.J. Strassler and C.-I. Tan, *On the eikonal approximation in AdS space*, *JHEP* **03** (2009) 050 [arXiv:0707.2408] [SPIRES].

[67] E. Levin, J. Miller, B.Z. Kopeliovich and I. Schmidt, *Glauber-Gribov approach for DIS on nuclei in* $N = 4$ *SYM*, *JHEP* **02** (2009) 048 [arXiv:0811.3586] [SPIRES].

[68] L. Cornalba, M.S. Costa and J. Penedones, *Eikonal approximation in AdS/CFT: resumming the gravitational loop expansion*, *JHEP* **09** (2007) 037 [arXiv:0707.0120] [SPIRES].

[69] L. Cornalba, M.S. Costa, J. Penedones and R. Schiappa, *Eikonal approximation in AdS/CFT: conformal partial waves and finite N four-point functions*, *Nucl. Phys.* **B 767** (2007) 327 [hep-th/0611123] [SPIRES].

[70] L. Cornalba, M.S. Costa, J. Penedones and R. Schiappa, *Eikonal approximation in AdS/CFT: from shock waves to four-point functions*, *JHEP* **08** (2007) 019 [hep-th/0611122] [SPIRES].

[71] S. de Haro, S.N. Solodukhin and K. Skenderis, *Holographic reconstruction of spacetime and renormalization in the AdS/CFT correspondence*, *Commun. Math. Phys.* **217** (2001) 595 [hep-th/0002230] [SPIRES].

[72] A. Krasnitz, Y. Nara and R. Venugopalan, *Probing a color glass condensate in high energy heavy ion collisions*, *Braz. J. Phys.* **33** (2003) 223 [SPIRES].

JHEP05(2009)060

[73] J.L. Albacete, Y.V. Kovchegov and A. Taliotis, *DIS on a large nucleus in AdS/CFT*, *JHEP* **07** (2008) 074 [arXiv:0806.1484] [SPIRES].

[74] U.H. Danielsson, E. Keski-Vakkuri and M. Kruczenski, *Vacua, propagators and holographic probes in AdS/CFT*, *JHEP* **01** (1999) 002 [hep-th/9812007] [SPIRES].

[75] P.M. Chesler and L.G. Yaffe, *Horizon formation and far-from-equilibrium isotropization in supersymmetric Yang-Mills plasma*, arXiv:0812.2053 [SPIRES].

JHEP05(2009)060